Nano Research

Open Access

Review Article

DNA-based plasmonic nanostructures with tailored optical responses

Renjie Niu[1,2], Jiale Du[1], Wenqing He[1], Bing Liu[1,3] ✉, and Jie Chao[1] ✉

[1] *State Key Laboratory for Organic Electronics and Information Displays & Jiangsu Key Laboratory for Biosensors, Institute of Advanced Materials (IAM), Jiangsu National Synergistic Innovation Center for Advanced Materials (SICAM), Nanjing University of Posts and Telecommunications, Nanjing 210023, China*
[2] *School of Medical Imaging, Xuzhou Medical University, Xuzhou 221004, China*
[3] *School of Medicine, Nanjing University of Chinese Medicine, Nanjing 210023, China*

Cite this article: *Nano Research*, **2025**, *18*, 94907197. https://doi.org/10.26599/NR.2025.94907197

ABSTRACT: Plasmonic nanostructures, particularly those composed of noble metals such as gold and silver, have garnered extensive attention due to their exceptional physical and chemical properties, which are highly advantageous for optical sensing applications. The unique characteristics of DNA enable the precise spatial arrangement and functionalization of nanoparticles, allowing for the tailoring of optical characteristics within plasmonic systems. This review encompasses the development of DNA nanotechnology and its application in constructing plasmonic nanostructures featuring diverse geometric configurations. It emphasizes the tailored optical responses of these structures, including surface-enhanced Raman scattering (SERS), fluorescence enhancement, and chirality. The review concludes with a discussion of the opportunities and challenges facing DNA-based plasmonic nanostructures.

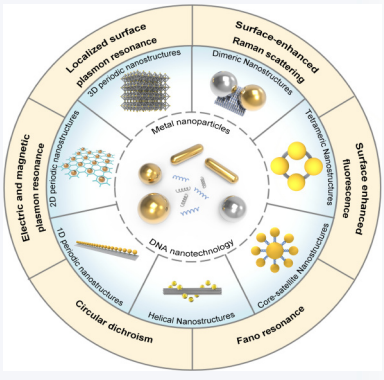

KEYWORDS: DNA nanotechnology, self-assembly, plasmonic nanostructures, optical responses

1 Introduction

Plasmonic nanostructures exhibit a variety of unique optical properties, such as localized surface plasmon resonance (LSPR), surface-enhanced Raman scattering (SERS), and chirality [1–4]. These characteristics have garnered significant attention in fields such as bioimaging, biosensing, therapeutics, and catalysis [5–7]. The optical response of plasmonic nanostructures is highly sensitive to subtle changes in parameters such as the material composition, size, interparticle gap, and nanoparticle shape [8]. Therefore, the precise spatial arrangement of metal nanoparticles is crucial for constructing advanced plasmonic nanostructures with tailored optical responses and novel functionalities. Although top-down lithographic methods are widely used to fabricate metal nanostructures with precise positioning and shapes, they are limited by resolution constraints, making it challenging to achieve sub-5 nm gaps [9]. Additionally, these methods often involve high equipment costs, complex fabrication steps, and difficulties in realizing intricate three-dimensional (3D) nanostructures [10].

The emergence of DNA nanotechnology provides new strategies for bottom-up large-scale and complex assembly of plasmonic nanostructures [11]. Beyond serving as genetic material, DNA has recently been recognized as promising building materials to arrange a variety of molecules and nanoparticles. The excellent properties of DNA nanostructures, such as programmability, sequence specificity, and structural plasticity, render them ideal assembly platforms with precise controllability, spatial addressability and target recognition [12]. In particular, structural DNA, such as DNA origami, provides highly programmable templates to assemble molecules and nanoparticles into precise patterns with nanometer-scale addressability [13]. This capability allows for the fine-tuning of plasmonic nanostructures, including the manipulation of interparticle spacing and structural configurations, which in turn enables the generation of tailored optical responses. These precise structural controls are crucial for tailoring the optical properties of plasmonic systems, thereby enhancing their potential in biological analysis.

In recent decades, a wide variety of DNA-based plasmonic nanostructures have been developed, ranging from discrete nanostructures to periodic nanoparticle arrays [14, 15]. These include dimers, tetramers, core-satellite structures, helical

Received: October 31, 2024; **Revised:** December 15, 2024
Accepted: December 16, 2024

✉Address correspondence to Jie Chao, iamjchao@njupt.edu.cn; Bing Liu, bingliu@njucm.edu.cn

structures, and one-, two-, and three-dimensional (1D, 2D, and 3D) arrays, all of which play crucial roles in the field of optical sensing [16–19]. This review focuses on the construction and optical applications of plasmonic nanostructures assembled via DNA. First, it briefly introduces the overview of development of DNA nanotechnology, tracing its evolution from its genetic material to a versatile tool for nanoscale material manipulation. DNA's unique properties, such as Watson–Crick base-pairing and tunable length, enable precise control over the spatial arrangement of nanoparticles, facilitating the creation of well-defined plasmonic nanostructures. Subsequently, the review provides a detailed analysis of the construction of plasmonic nanostructures with different geometric configurations. It examines the relationship between these configurations and their diverse optical responses, emphasizing how the geometry of plasmonic nanostructures is intrinsically linked to their optical properties. By categorizing DNA-based plasmonic nanostructures according to their geometric configurations, the review offers insights into their tailored optical responses. Finally, we summarize the advantages of DNA-based plasmonic nanostructures, along with the current opportunities and challenges they encounter. This review aims to provide researchers with a comprehensive overview of DNA-based plasmonic nanostructures with tailored optical responses, thereby assisting them in their future research endeavors.

2 The development of DNA nanotechnology

The field of DNA nanotechnology was pioneering by Seeman who first proposed using DNA as a molecular building material in 1982 [20]. He believed that DNA branched junctions with complementary sticky ends could be utilized to construct 3D crystalline materials. However, these branched junctions have limitations including geometric flexibility and instability. To address these challenges, more rigid DNA structures, such as double-crossover (DX) molecules, were developed [21]. DX molecules consist of two side-by-side double-stranded helices connected at two crossover junctions. Using these molecules, researchers assembled the first striped 2D DNA lattice and created the first DNA nanomechanical device [22, 23]. On this foundation, structural DNA nanotechnology flourished, leading to developments of triple-crossover (TX) structures, cross motifs, three-point and six-point star motifs, tensegrity triangles, and T-junctions. These constructs were employed to create deliberately designed geometric shapes and highly ordered 2D crystals [24–27]. Later, Shih et al. fabricated a DNA octahedron by folding a long single-stranded DNA molecule with five synthetic 40-mer oligodeoxynucleotides (Fig. 1(a)) [28]. This method likely inspired the DNA origami techniques that followed.

In 2006, the advent of DNA origami represented a significant breakthrough in structural DNA nanotechnology. This technique involves folding a single-stranded DNA scaffold, which is fixed by hundreds of short staple strands, into arbitrary 2D shapes, such as triangles, rectangles, stars, and other designed patterns (Fig. 1(b)) [29]. In the following years, researchers advanced DNA origami to produce complex 3D structures (Fig. 1(c)) and larger-scale assemblies [30, 31]. DNA origami is characterized by high yield, a straightforward assembly process, and ease of purification. Most importantly, each DNA origami structure contains hundreds of addressable sites, offering superior stability and complexity compared to earlier DNA structures [32–35]. Additionally, computer programs can be utilized to simplify the design process of DNA origami [36, 37]. These unique properties make DNA origami an excellent template for assembling nanomaterials, such as metal nanoparticles and proteins.

The development of structural DNA nanotechnology made progress in 2012 when Yin et al. introduced the use of single-stranded tiles (SST) to construct 2D and 3D shapes (Fig. 1(d)) [38, 39]. This technique achieves complexity comparable to DNA origami but does not necessitate a long scaffold strand. Instead, hundreds of short single strands are assembled into intricate DNA nanostructures. Each single-stranded tile contains a fixed number of bases and is composed entirely of concatenated sticky ends. During self-assembly, each tile is complementary to the four surrounding DNA strands, allowing it to be independently added or removed. Since all sequences are unique, a master collection of strands corresponds to a molecular canvas, where the complementary regions of adjacent DNA strands represent a pixel or voxel. By selecting specific pixels or voxels, virtually any desired shape can be created.

With the rapid development of static DNA nanostructures, numerous dynamic DNA nanomachines have been constructed [40–43]. In 2000, a seminal paper first introduced the concept of isothermal DNA strand displacement [44]. This technique allows molecular tweezers open and close by the addition of auxiliary "fuel" DNA strands. The strand displacement reaction was later applied to more complex DNA machines, facilitating the transformation of precursor DNA nanocages into intricate nanocages [45]. Over time, dynamic DNA nanomachines driving by various forces have been developed over time. In 2015, Dietz's group designed 3D DNA components capable of switching between different structural states through three distinct methods: (i) Altering the cation concentration, (ii) changing the solution temperature, and (iii) strand displacement reactions [46]. Recently, dynamic DNA origami has been widely applied to drug-responsive release [47]. For example, our group designed an intelligent DNA nanodevice for precision thrombolysis, emphasizing the dynamic transformation between tubular and rectangular DNA origami structures [48]. The device utilizes a thrombin-responsive mechanism, where a tubular DNA structure transitions into a rectangular form upon detecting thrombin. This transformation is facilitated by interlocking DNA triplex structures that act as a computing core, controlling the release of tissue plasminogen activator (tPA) only when thrombin concentrations levels exceed a specific threshold. This dynamic structural change ensures targeted drug delivery, minimizing off-target effects. Kim et al. utilized the mechanism of paper folding to create reconfigurable DNA origami. By designing reference planar wireframe structures, they ensured that the edges followed the crease patterns of paper folding, thereby achieving folding into various target shapes. They demonstrated the reversibility, repeatability, and reliability of these DNA origami in response to different environmental stimuli and explored their potential applications in molecular sensors and fluorescence signal control (Fig. 1(e)) [49].

3 DNA-based plasmonic nanostructures

The self-assembly of nanomaterials with nanometer-level precision is one of the important challenges in nanotechnology [50], involving various materials such as metal nanoparticles, fluorescent dyes, carbon nanotubes, and biological materials [51–53]. DNA provides novel strategies for assembling well-defined nanostructures. In particular, the high rigidity, high assembly yield,

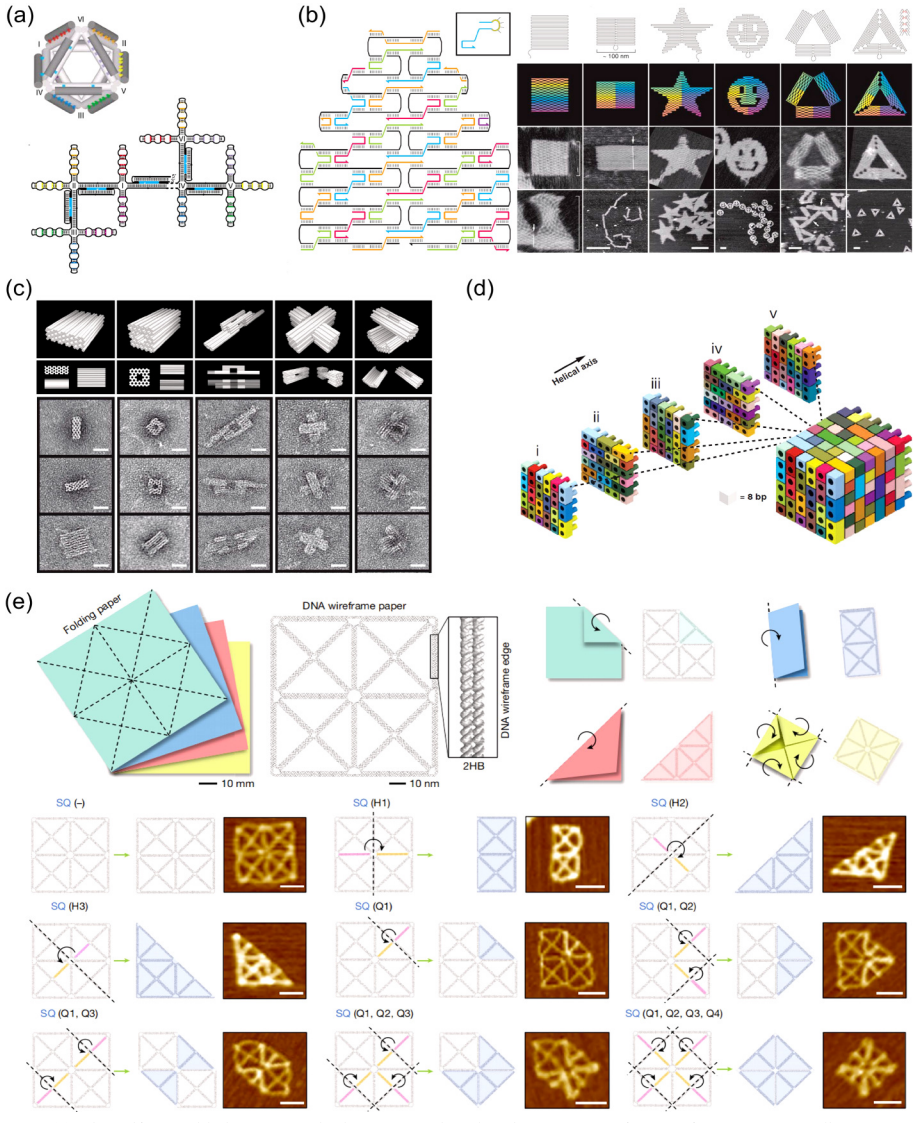

Figure 1 DNA nanostructures. (a) The self-assembled DNA octahedron. Reproduced with permission from Ref. [28], © Macmillan Magazines Ltd 2004. (b) Different shapes of 2D DNA origami. Reproduced with permission from Ref. [29], © Springer Nature Limited 2006. (c) Different shapes of 3D DNA origami. Reproduced with permission from Ref. [30], © Macmillan Publishers Limited. All rights reserved 2009. (d) 3D shapes self-assembled from single-stranded DNA tiles. Reproduced with permission from Ref. [38], © American Association for the Advancement of Science 2012. (e) Reconfigurable DNA origami based on paper folding mechanism. Reproduced with permission from Ref. [49], © Kim, M. et al. under exclusive licence to Springer Nature Limited 2023.

and addressability of DNA origami make it an excellent template for the precise arrangement of nanoparticles, enabling the construction of well-defined nanostructures. Over the past few decades, a wide variety of nanoparticle assemblies have been produced, ranging from discrete nanostructures to dimensionality-confined and bulk nanoparticle arrays. Given the geometric configurations of plasmonic nanostructures are closely linked to their optical properties, this section will categorize DNA-based plasmonic nanostructures according to their different geometrical configurations. It will analyze the assembly methods and optical properties of various structures, including discrete and periodic nanostructures. By exploring these configurations, we aim to provide insights into the tailored optical responses and potential applications of these innovative assemblies.

3.1 Discrete nanoparticle assemblies

In recent years, the controllable assembly of discrete nanostructures has garnered significant research attention due to its immense potential in fundamental physics and the development of functional nanodevices. Traditional assembly methods primarily relied on covalent "linker" molecules, which presented challenges such as difficulty in process control and irreversible component formation. In 1996, Alivisatos et al. pioneered the use of DNA for the controllable assembly of nanoparticles into discrete nanostructures [54]. By attaching single-stranded DNA of specific lengths and sequences to individual nanoparticles, they successfully assembled these into dimers and trimers through the addition of complementary single-stranded DNA. This approach demonstrated that DNA could be utilized to assemble functional colloidal nanoparticles into well-defined nanostructures with intriguing properties, while also allowing for reversibility in the assembly process. This innovation symbolized the beginning of a new era in DNA-based nanoparticle self-assembly. This section will delve into the discrete nanoparticle assemblies precisely constructed using

DNA nanotechnology, highlighting their unique properties and potential applications.

3.1.1 *Dimeric nanostructures*

Among the various nanoparticle assemblies, the dimers, composed of two nanoparticles, are the most basic and straightforward nanostructures. Compared to more complex configurations, dimers have the advantages of easy assembly and high yield.

3.1.1.1 Homodimeric nanostructures

The homodimers, consisting of identical nanoparticles are one of the simplest forms of dimeric nanostructures. Initially, basic DNA structures, such as double-stranded DNA or DNA stem loops, are used to construct these dimeric assemblies [55]. For example, Chen et al. demonstrated the assembly of two gold nanoparticles (AuNPs) into a dimer using a DNA hairpin loop, positioning the nanoparticles in close proximity. Upon the introduction of a target strand complementary to the hairpin sequence, the loop was disrupted, causing the stretch of DNA and an increase in the nanogap. This change in distance between the nanoparticles affected the energy of the LSPR modes. As the DNA structure expanded, the increased distance between the particles elevated the energy of the coupled plasmonic modes, resulting in a blue shift of the dimer's scattering resonance (Fig. 2(a)) [56].

In addition to AuNPs, the application of assembling gold nanorods (AuNRs) through simple DNA structures is also extensive [57]. For example, Tang et al. investigated the enhancement of SERS signals by constructing AuNR dimers [58]. The researchers first assembled the AuNRs into dimers through DNA hybridization and then coated their surfaces with silver shells to further amplify the SERS signal. The silver shell not only reduced the gap between the AuNRs but also significantly enhanced the Raman signal. Experimental results showed that as the silver shell thickness increased, the SERS signal intensity initially increased and then decreased, with the optimal thickness achieved using 2.5 mM $AgNO_3$. At this thickness, the SERS signal intensity was approximately six times higher than that of dimers without the silver coating. Using this approach, they developed an ultra-sensitive and highly selective method for dopamine detection (Fig. 2(b)). In the same year, they developed a similar method for detecting prostate-specific antigen (PSA). The PSA aptamer (DNA1) and its complementary fragment (DNA2) were attached to the sides of AuNRs, forming AuNR dimer probes through hybridization. The circular dichroism (CD) signals were amplified by depositing silver shells on the surface of the AuNR dimers. Upon the addition of PSA, the dimers dehybridized to form monomers. As the concentration of PSA increased, the CD intensity decreased [59].

With the development of DNA nanotechnology, complex DNA nanostructures such as DNA origami are prone to use for nanoparticles assembly because of their precise addressability. DNA origami can precisely control the patterns of nanoparticle assembly.

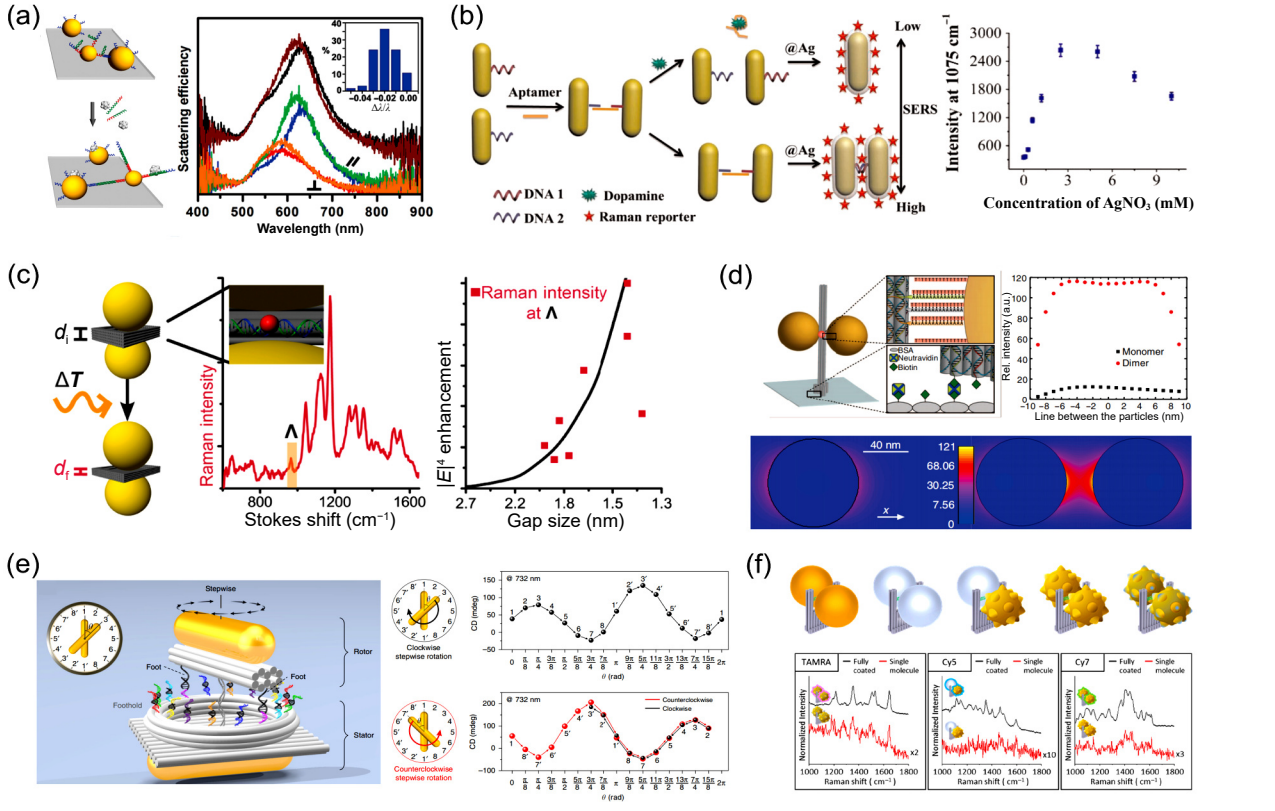

Figure 2 Dimeric nanostructures. (a) Assembly of AuNP dimers via DNA hairpin loop and their LSPR mode energy variations. Reproduced with permission from Ref. [56], © American Chemical Society 2010. (b) Silver-coated AuNR dimers significantly enhance SERS signals. Reproduced with permission from Ref. [58], © Elsevier B.V. All rights reserved 2015. (c) AuNP dimers with precisely controlled gaps and their tunable SERS signals. Reproduced with permission from Ref. [60], © American Chemical Society 2016. (d) AuNP dimers significantly enhance fluorescence. Reproduced with permission from Ref. [67], © American Association for the Advancement of Science 2012. (e) 360° rotating AuNR dimers and their dynamic CD signal monitoring. Reproduced with permission from Ref. [69], © Xin, L. et al. 2019. (f) Au/Ag nanoparticle dimers optimize SERS for single-molecule detection with broadband excitation across the visible spectrum. Reproduced with permission from Ref. [76], © Kanehira, Y. et al. Published by American Chemical Society 2023.

For example, Simoncelli et al. utilized DNA origami to construct AuNP dimers, with the DNA origami template designed to precisely position single or multiple dye molecules at the geometric center of the dimer, and to accurately control the gap size between the AuNPs. By adjusting the dimer gap size, the wavelength of its plasmonic resonance can be altered. As the gap narrowed from 3.3 to 1.3 nm, a redshift in the plasmon resonance peak occurred, indicating enhanced plasmon coupling and significantly increase in SERS signals intensity. This study demonstrates the ability of DNA origami to precisely manipulate nanoparticle gaps, thereby modulating optical properties and enabling single-molecule-level SERS signal detection (Fig. 2(c)) [60]. Dimer structures are frequently employed to enhance Raman signals because they can form intense electromagnetic field enhancement regions, known as "hot spot" in the gaps between two nanoparticles, significantly boosting the intensity of Raman signals [61–66]. In addition to amplifying the Raman signal, the same electromagnetic field enhancement mechanism can be applied to other optical phenomena, such as fluorescence enhancement, to boost the signals intensity. In 2012, Tinnefeld and co-workers constructed a nanoantenna by attaching two AuNPs to a DNA origami template and simultaneously positioning a single fluorescent dye in the gap between the AuNPs. They tested the dependence of fluorescence intensity on the size and number of AuNPs, achieving a remarkable 117-fold increase in fluorescence of the 100 nm dimers (Fig. 2(d)) [67]. This development paved the way for sensor applications and nano-scale light control, extending the range of single-molecule measurements to biologically relevant micromolar concentration.

Moreover, DNA origami enables the achievement of complex dynamic changes in nanoparticle assemblies, allowing the optical properties of dynamic plasmonic systems to be actively manipulated. In 2017, Ding and colleagues constructed a dynamic plasmonic nanostructure that effectively responded to various stimuli. They assembled AuNRs into an L-shaped configuration on a spliced rhombus-shaped DNA origami. This structure responded to multiple stimuli, including glutathione reduction, restriction enzyme action, pH changes, and photoirradiation. Glutathione reduction and restriction enzyme activity caused irreversible changes in CD signals, while pH changes and photoirradiation triggered reversible alterations in CD signals [68]. In addition to external stimuli, the toehold-mediated strand displacement reaction is the most common method. For instance, Liu and colleagues developed a rotary plasmonic nanoclock assembled by DNA origami (Fig. 2(e)) [69]. In this system, the rotor AuNR could be directionally and reversibly rotated 360° relative to the stator AuNR through the strand displacement reaction. The entire rotational process was monitored in real-time using CD signals. This work laid the foundation for developing DNA-assembled nano-optical systems with dynamic complexity and tailored optical functions. AuNRs are frequently employed in the constructing of chiral structures [70], owing to their rod-like shape, giving them significant practical utility in various biological and chemical applications. For example, Ding and colleagues constructed a dynamic AuNR dimer. When specific input signals were present—such as nucleic acids, adenosine, chiral tyrosamine, or specific receptors expressed on the surfaces of tumor cells—they used DNA logic circuits as recognition and amplification elements to generate DNA keys that drove conformational changes in the AuNR dimers. These changes enabled the sensitive detection and amplification of weak biological or chemical signals through significant alterations in the CD signals. This system had potential applications in biosensing, diagnostics, and the amplification of sensitive biological signals [71].

3.1.1.2 Heterodimeric nanostructures

In addition to homodimers, heterodimers consisted of two nanoparticles differing in sizes, shapes, or materials have attracted great interest due to their ability to induce complex optical responses [72]. Initially, nanomaterials of the same type but different sizes were introduced by Lim et al. High-yield heterodimers by DNA hybridization between two AuNPs of different sizes and a dye molecule were successfully synthesized. The dye molecule was strategically assembled between the two particles, which was the hot spot region. By depositing silver shells on the surfaces of AuNP dimers and controlling the shell thickness, gap-tailorable gold-silver core-shell nanodumbbells (GSNDs) were produced. Raman signals were detected by Raman spectroscopy coupled with atomic force microscope (AFM). These GSNDs with Raman-active can be further modified by other biomolecules, serving as *in vitro* and *in vivo* bio-labelling probes with ultra-high sensitivity, quantitative potential and multiplexing capabilities. This work has paved the way for advancement in single-molecule detection and biological assays [73]. Subsequently, Hao et al. assembled the two shapes of nanoparticles to construct AuNP-AuNR heterodimers with chiral molecules for the first time by DNA hybridization and explored its chiral activity. The heterodimers composed of two differently shaped nanoparticles, utilized three different sizes of AuNRs. By adjusting the component sizes, the heterodimers showed a systematic variation in the intensity and wavelength of the CD signals, which reflected a tailored chiral response. This study provided a new opportunity to create heterogeneous nanoscale plasmonic objects with customized chiroptical responses for applications in biosensors and chiral medical carriers [74]. The exploration of nanomaterials with different element compositions is gaining momentum. Baumberg and co-workers used DNA origami technology to assemble 40 nm AuNPs and 40 nm silver nanoparticles (AgNPs) into Au-Ag heterodimers. The 5 nm gap between two particles enabled direct dipole coupling of Au and Ag electrons. There polarization-dependent response was characterized in detail, revealing consistency with their heterocomponent nature and broken symmetry. This work holds important potential for experimental research on complex geometric structures such as metals, semiconductors, and dielectrics [75]. DNA origami has been utilized to construct different shapes of heterocomponent dimer. The plasmonic nanoantenna structure is composed of Au and Ag nanoparticles, incorporating spherical and flower-shaped designs (Fig. 2(f)) [76]. The shape and arrangement of the nanoparticles directly influence the LSPR properties and the enhancement of SERS signals. Therefore, researchers have precisely controlled the assembly process to design five different plasmonic nanoparticle dimer configurations, optimized to match specific SERS excitation wavelengths. These heterogeneous dimers exhibit unique LSPR characteristics, particularly enhanced the "hot spot" intensity generated at the sharp edges of the flower-shaped structures, significantly improving the potential for single-molecule SERS. By forming heterogeneous dimer structures between Au and Ag nanoparticles, broadband excitation covering the entire visible spectrum is achieved. Additionally, the study explores extinction and near-field properties, finding that surface roughness significantly alters the extinction spectrum and enhances field strength.

3.1.2 *Tetrameric nanostructures*

DNA-based plasmonic nanostructures became more complex by assembling multiple nanoparticles. Among these, tetrameric nanostructures form a unique and expansive system due to their ability to achieve chiroptical properties [77, 78]. The chirality of biological entities can be traced back to the tetrahedral geometry of sp^3-hybridized carbon atoms with four different substituents. In 2009, the development of chiral tetrahedrons, also known as pyramid structures, initiated research into using DNA to assemble chiral superstructures [79]. Therefore, this section will be divided into two parts: pyramid nanostructures and other tetrameric nanostructures.

3.1.2.1 Pyramid nanostructures

In 2009, Alivisatos and co-workers constructed discrete pyramid nanostructures, employing double-stranded DNA as a scaffold to precisely position AuNPs. The unique sequence of each DNA strand allowed for the placement four sizes of particles grafted at the end of each strand to build these chiral nanostructures, although the chiral properties based on this formation were not reported [79]. The first DNA-based nanosrutures demonstrated strong chiroptical activity were constructed by Yan et al. They introduced a high-yield method for preparing chiral pyramids composed of multiple metal and/or semiconductor nanoparticles (Fig. 3(a)) [80]. The chiral pyramids, designed as R- and S-enantiomers, and assembled from three different materials. Notably, each NP component contributed to this chiroptical activity, allowing the simultaneous observation of three distinct circular dichroism signals within the 350–550 nm range. The chiral nanodevice was also applied to biology. Sun et al. developed a yolk-shell nanoparticle (YSNP) pyramid incorporating an upconversion nanoparticle (UCNP) at its center. This chiral nanodevice was used to induce autophagy *in vivo* and demonstrated adjustable circular dichroism signals when modified with different glutathione enantiomers, holding its potential in cell biology [81]. Beyond chiral properties, pyramid nanostructures have applications in other fields. For instance, in 2015, Xu et al. constructed DNA-driven AgNP pyramids capable of ultra-sensitive, simultaneous detection of multiple quantitative disease biomarkers. These AgNP pyramids were engineered using a DNA framework embedded with biomarker-specific aptamers. In the presence of a target biomarker, the pyramid's 3D geometric configuration would shift, shortening the gap length due to the specific biomarker-aptamer interactions. This structural adjustment enhanced Raman signals, establishing a foundation for developing versatile disease biomarker detection protocols [82].

3.1.2.2 Other tetrameric nanostructures

In addition to pyramid structures, Ding and co-workers used rectangular DNA origami templates to organize four identical AuNPs into 3D asymmetric tetramers with high precision (Fig. 3(b)) [83]. The chiral nanostructures, consisted of the minimum number of spherical AuNPs required for a 3D chiral formation, and results in significant CD. At the corners of a rectangular DNA origami, four AuNPs were selectively positioned and amplified through solution metal deposition, resulting in assemblies with "hot spots" of enhanced electromagnetic fields. This configuration significantly boosted the Raman signals of attached molecules [84]. Similarly, Liedl and co-workers controllably placed four AuNPs on 3D circular DNA origami to produce plasma supramolecules. The unique characteristics of the plasma were analyzed by single-ring scattering spectra and the absorption spectra of metamolecules solutions, showcasing that the electric and magnetic plasmon resonance modes are closely related to the structure shapes (Fig. 3(c)) [85]. AuNPs of different sizes were assembled on two sides of triangular DNA origami by our group to construct right and left-handed chiral tetramer nanostructures [86]. To reduce the charge repulsion between the DNA templates and nanoparticles, we later developed a hole-type DNA origami, arranging 30 nm AuNPs into dimer and tetramer plasmonic nanostructures, which exhibited significant Raman signals [87]. For assembly of large AuNPs, Fang et al. utilized super-origami DNA framework to fix them at designated n-tuple docking sites. These tetrameric nanoclusters, each comprising four spatially organized 80 nm AuNPs, exhibited peak-dip Fano characteristics. These structures generated strong electromagnetic field "hot spots" at the Fano resonance wavelength, significantly enhancing single-molecule SERS. This setup enabled the quantitative analysis of SERS signals from individual dye

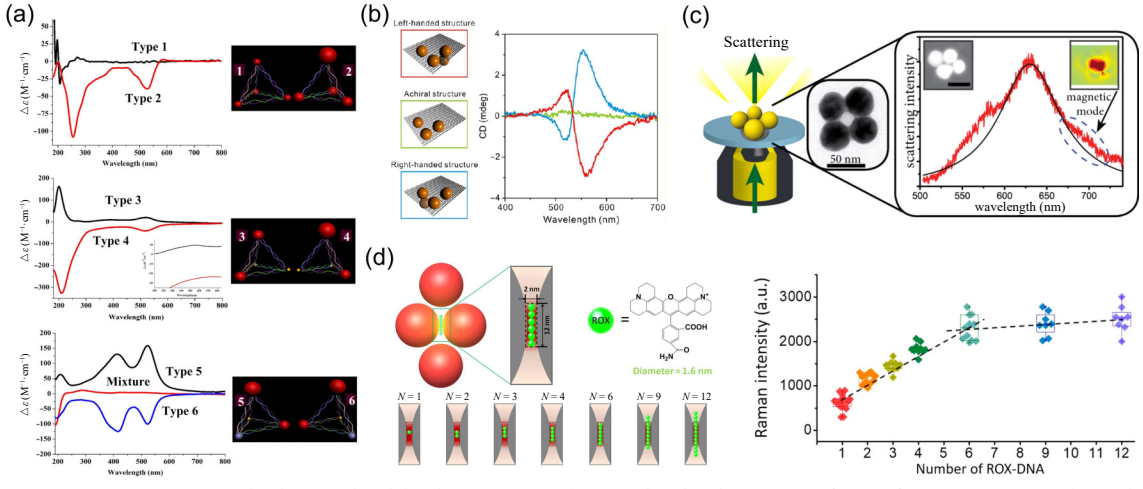

Figure 3 Tetrameric nanostructures. (a) Chiral pyramids exhibit distinct CD signals. Reproduced with permission from Ref. [80], © American Chemical Society 2012. (b) 3D asymmetric AuNP tetramers with significant CD. Reproduced with permission from Ref. [83], © American Chemical Society 2013. (c) AuNP Rings exhibit electric and magnetic resonances at visible frequencies. Reproduced with permission from Ref. [85], © American Chemical Society 2015. (d) AuNP tetramers and the quantitative analysis of SERS signals from single dye molecules. Reproduced with permission from Ref. [88], © Fang, W. N. et al. some rights reserved; exclusive licensee American Association for the Advancement of Science 2019.

molecules, providing an ideal platform for ultra-sensitive sensing and single-molecule biophysical studies (Fig. 3(d)) [88].

3.1.3 *Core-satellite nanostructures*

Core-satellite structures, multi-component assemblies, have garnered significant attention for their unique optical properties and versatility. Typically, they consist of a central core particle surrounded by smaller satellite particles, forming a layer configuration. The proximity between the core and satellite nanoparticles induces LSPR, resulting in strong coupling plasmon resonance bands. These unique optical properties have captivated researchers due to their applications in SERS probes, plasmon resonance scales, optical sensors, and biological transport and elimination. In 1998, Letsinger and co-workers pioneered the use of DNA-directed assembly to construct core-satellite structures, forming network architectures and paved the way for DNA nanotechnology in building such nanostructures [89].

3.1.3.1 Isotropic core-satellite nanostructures

Isotropic core-satellite nanostructures are characterized by symmetrical arrangement of satellite particles around a central core, resulting in uniform optical properties in all directions. In 2017, Ma et al. developed a core-satellite nanostructure composed of AuNR dimers and UCNPs (Fig. 4(a)) [90]. Constructed on a DNA framework, these structures exhibited dual SERS and luminescence signals. The AuNR dimers demonstrated strong SERS activity within nanoscale gaps, while the UCNPs were quenched through a luminescence resonance energy transfer process. This dual functionality enabled ultra-sensitive quantitative detection of intracellular miR-21 and telomerase. Later that year, the same group produced a multifunctional nanostructure composed of AuNR-Pt and Ag_2S core-satellite assemblies. This nanostructure was designed for the quantification of intracellular miR-21, near-infrared fluorescent cell imaging, and *in vivo* tumor ablation [91]. In 2019, He et al. developed a method to accurately manipulate DNA density on the surface of AuNPs, resulting in a core-satellite nanostructure with excellent stability and enhanced SERS signal through controlled hot spots. This highly ordered configuration enabled SERS-based miRNA detection with low background interference, showcasing its reliability in molecular diagnostics [92]. The particle density on the surface of AuNPs can be better controlled using DNA tetrahedra. Feng et al. assembled the satellite particles around a center core by DNA tetrahedra and applied SERS technology to design a molecular ruler for real-time monitoring of conformational changes in individual Hg^{2+} aptamers (Fig. 4(b)) [93]. This structure, combined with dark-field microscopy (DFM) and Raman spectroscopy, enables continuous observation of Hg^{2+}-induced conformational changes in aptamers, significant enhancing SERS signals. The conformational change events of the aptamers were further validated using *in-situ* scanning electron microscopy (SEM) and finite-difference time-domain (FDTD) calculations. Moreover, this SERS molecular ruler method effectively investigates the intermediate states, binding sites, and kinetics of conformational changes in aptamers. These findings provide fundamental insights into the mechanisms of DNA aptamer conformational changes and lay the groundwork for designing DNA aptamer-based biological applications.

3.1.3.2 Anisotropic core-satellite nanostructures

Anisotropic core-satellite nanostructures feature an asymmetrical arrangement of satellite particles around the core, resulting in direction-dependent optical properties that giving them anisotropic. Advances in DNA nanotechnology have enabled more precise control over the assembly of these core-satellite nanostructures [94–106]. Xu et al. discovered that at low DNA concentrations, DNA strands selectively attached to the ends of AuNRs, enabling the controlled assembly of AuNPs at either the ends or the sides of the AuNRs. They developed three configurations with modification the surface of AuNR with single-stranded DNA, resulting in three distinct core-satellite structures: end, side, and satellite. The SERS

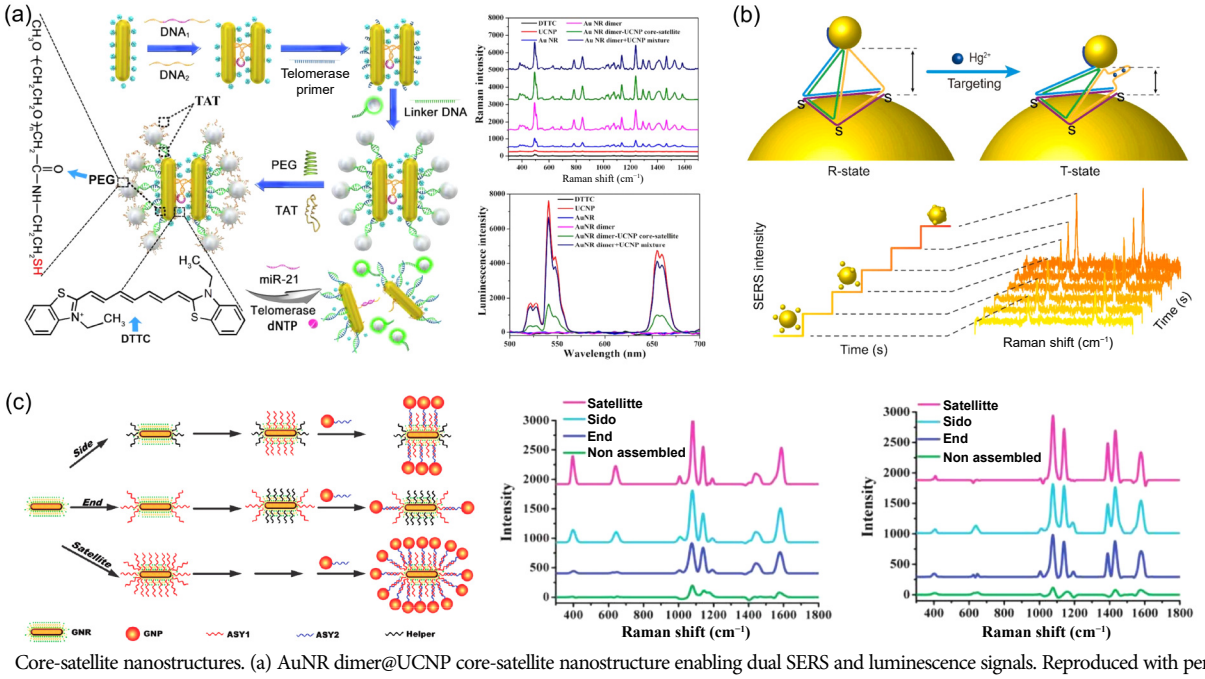

Figure 4 Core-satellite nanostructures. (a) AuNR dimer@UCNP core-satellite nanostructure enabling dual SERS and luminescence signals. Reproduced with permission from Ref. [90], © American Chemical Society 2017. (b) AuNP@AuNP core-satellite nanostructure serving as a molecular ruler using SERS technology for real-time monitoring of Hg^{2+} aptamer conformational changes. Reproduced with permission from Ref. [93], © Elsevier B.V. All rights reserved 2021. (c) Anisotropic AuNR@AuNP core-satellite nanostructures with varying SERS intensities. Reproduced with permission from Ref. [107], © American Chemical Society 2011.

intensity of these structures primarily depends on the number of AuNPs incorporated (Fig. 4(c)) [107]. Additionally, *in vivo* studies demonstrated that these structures can serve as unlabeled intracellular probes, providing real-time insights into local metabolic processes.

In the aforementioned core-satellite structures, precise control over the number and spatial positioning of the satellites remains challenging. Our group has pioneered a precise nanoparticle modification method known as DNA-origami-based nanoimprinting lithography. Leveraging the programmable addressing capabilities of DNA origami, we developed a platform analogous to a photocopier. Using DNA strand displacement reactions, DNA strands prearranged on the DNA origami are transferred onto the nanoparticle surface, allowing for precise control over the spatial position, quantity, and sequence of DNA strands. By assembling small AuNPs (satellites), we constructed various anisotropic core-satellite structures, including AuNP@AuNP, AuNR@AuNP, and AuNC@AuNP. For these diverse structures, CD and SERS signals were characterized according to their structural features, successfully achieving SERS signal detection at the single-molecule level [108–110]. Sleiman and co-workers developed a similar but distinct approach, termed molecular printing, to transfer DNA strands from a parent 3D DNA template to the surface of AuNPs, creating a range of anisotropic core-satellite structures [111]. In 2019, Xie et al. applied the molecular printing strategy to a 3D level using icosahedral DNA cages, to achieve precise control of AuNPs in 3D space, resulting in an even broader array of anisotropic core-satellite structures [112]. However, their research focused solely on structural construction without exploring the optical properties.

3.1.4 *Helical nanostructures*

Research on DNA-assembled chiral superstructures primarily focuses on two fundamental configurations: tetrahedrons and helices. While chiral tetrahedrons have been studied since 2009, helical structures have recently attracted more attention, likely due to the superior chiral properties. Kuzyk et al. were the first to demonstrate the role of structural DNA nanotechnology in constructing rigid plasmonic architectures (Fig. 5(a)) [113]. They used 3D rigid DNA origami with 24-helix bundles as templates to create left-handed and right-handed helical AuNPs structures. In solution, they exhibited distinct CD and optical dispersion effects at visible wavelengths, resulting from the collective plasmon-plasmon interactions among the nanoparticles. In another method developed by Shen et al., AuNPs were assembled along two parallel lines on 2D rectangular DNA origami. By rolling the rectangular DNA origami into tubes, AuNPs were automatically arranged into 3D helical structures that exhibited a measurable CD response in the visible spectrum [114]. Since then, the use of DNA origami to build helical structures has expanded [115–122].

Schreiber et al. investigated the CD signals of helical nanostructures on a glass substrate. They constructed left-handed nanohelices with a diameter of 34 nm, a helical pitch of 57 nm, and a total length of 79 nm by attaching 10 nm AuNPs to the surface of a rigid DNA origami 24-helix bundle. To enable upright alignment of nanohelices on a BSA-biotin-neutravidin-coated quartz glass surface, one end of the DNA origami was modified with 10 biotin molecules, positioning them parallel to the light beam. The quartz glass was subsequently dried with nitrogen and repositioned in an empty cuvette, causing the nanohelices to align parallel to the glass surface and perpendicular to the light beam. As expected, the CD signal changed according to the orientation of the left-handed nanohelices [123].

Unlike prior approaches, Cecconello et al. utilized self-assembled DNA barrels instead of DNA origami. The folding of the barrels was directed by initiator strands, which induced the assembly of right-handed or left-handed chains through electronic and/or spatial interactions. These chains then hybridized with functionalized AuNPs to produce chiralhelical structures. These structures exhibited distinct CD spectral features at visible

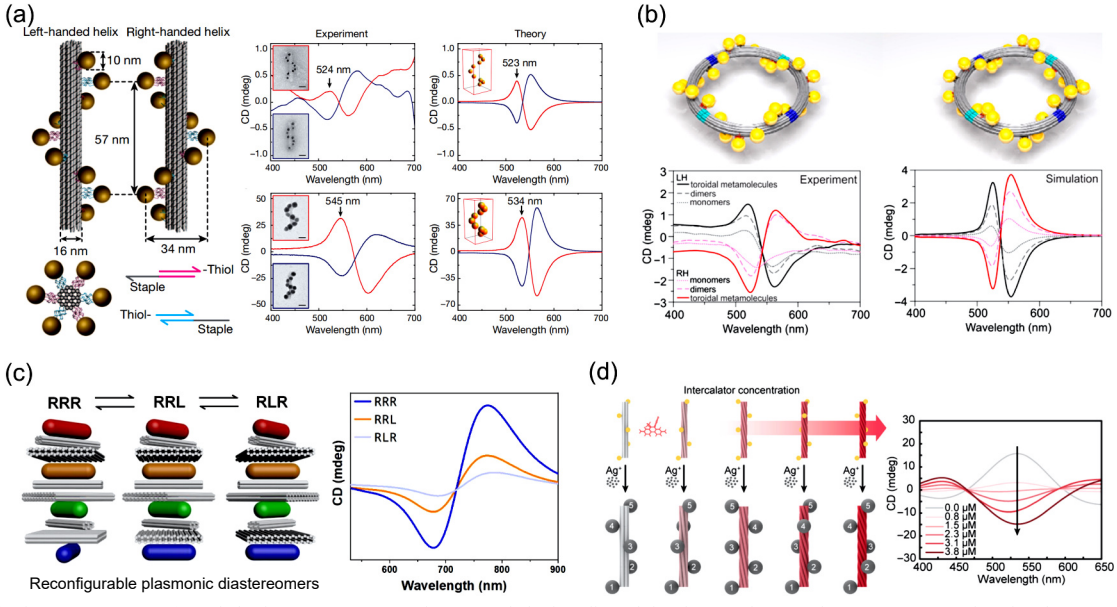

Figure 5 Helical nanostructures. (a) 3D helical AuNPs constructed using 24-helix bundles exhibit distinct chiroptical properties. Reproduced with permission from Ref. [113], © Springer Nature Limited 2012. (b) Circular helical structures and their CD signals. Reproduced with permission from Ref. [125], © American Chemical Society 2016. (c) Reconfigurable plasmonic AuNR helices exhibit enhanced CD signals. Reproduced with permission from Ref. [126], © American Chemical Society 2019. (d) Controlled chiroptical responses via DNA intercalators, with Ag enhancement amplifying and stabilizing the signal. Reproduced with permission from Ref. [127], © American Chemical Society 2024.

wavelengths, due to plasmonic coupling between the nanoparticles. Furthermore, the CD signal of the left-handed structures was stronger than that of the right-handed ones, which might be attributed to the overall twist of the DNA barrel scaffold [124].

In addition to rod-shaped helical nanostructures, Liu and co-workers constructed circular helical structures of plasmonic toroidal metamolecules by the layered assembly (Fig. 5(b)) [125]. Each toroidal metamolecule comprised four identical DNA origami-AuNP helical building blocks. Due to the symmetry of the toroidal structure, a unique chiroptical response along the axis could be observed by rotating the metamolecule coating on substrates. Compared to monomers and dimers, these tetrameric toroidal metamolecules exhibit significantly stronger chiroptical responses.

Beyond AuNPs, AuNRs can also be used to construct chiral helices. In 2019, Wang et al. employed 3D DNA origami for the hierarchical assembly of reconfigurable plasmonic AuNR helices, where each chiral center could be independently switched between left-handed and right-handed states. Using these plasmonic diastereomers, the study demonstrated strong near-field coupling between the chiral centers, which significantly enhanced the overall CD signal (Fig. 5(c)) [126].

Instead of being triggered by chemical reactions, various chiroptical responses can be controlled through chemo mechanical deformation induced by DNA intercalators (Fig. 5(d)) [127]. The chiroptical response could be precisely adjusted by altering the concentration of the intercalators. Ag enhancement technology was applied to amplify the chiroptical signal by enlarging the nanoparticles and reinforcing the template DNA structure.

3.1.5 *Other nanostructures*

Beyond the representative nanostructure's configurations mentioned previously, DNA nanotechnology enables the formation of many complex and novel discrete nanostructures [128–132]. Here are some typical examples.

Trimeric nanostructures also exhibit excellent optical properties. For instance, Ke and co-workers precisely positioned AuNRs on a reconfigurable DNA origami tripod to create a 3D plasmonic trimer. Through toehold-mediated strand displacement, they accurately adjusted the angles and distances between AuNRs, leading to controllable shifts in plasmonic resonance peaks, as observed by DFM and consistent with electrodynamic calculations (Fig. 6(a)) [133]. Nanolenses, consists of self-similar chains of differently sized spherical particles, generate giant local fields through cascaded enhancement. Bald's team assembled AgNPs of varying sizes (10, 20, and 60 nm) on triangular DNA origami surfaces to form silver nanolenses. A single streptavidin protein tagged with an alkyne group was selectively integrated into the gap with the highest electric field enhancement, serving as a model analyte for the SERS experiment. Its presence was confirmed through Raman mapping and AFM, revealing the SERS signal of a single streptavidin within an individual silver nanolens (Fig. 6(b)) [134]. Trimers can also exhibit chirality changes. Fan and co-workers designed a tetrahedral DNA origami template to hybridize AuNRs, utilizing the proton-responsive DNA strands to enable the self-assembly of AuNRs into plasmonic supramolecules with various spatial configurations. This approach successfully achieved 11 distinct configurations, including 4 trimers, and controlled the

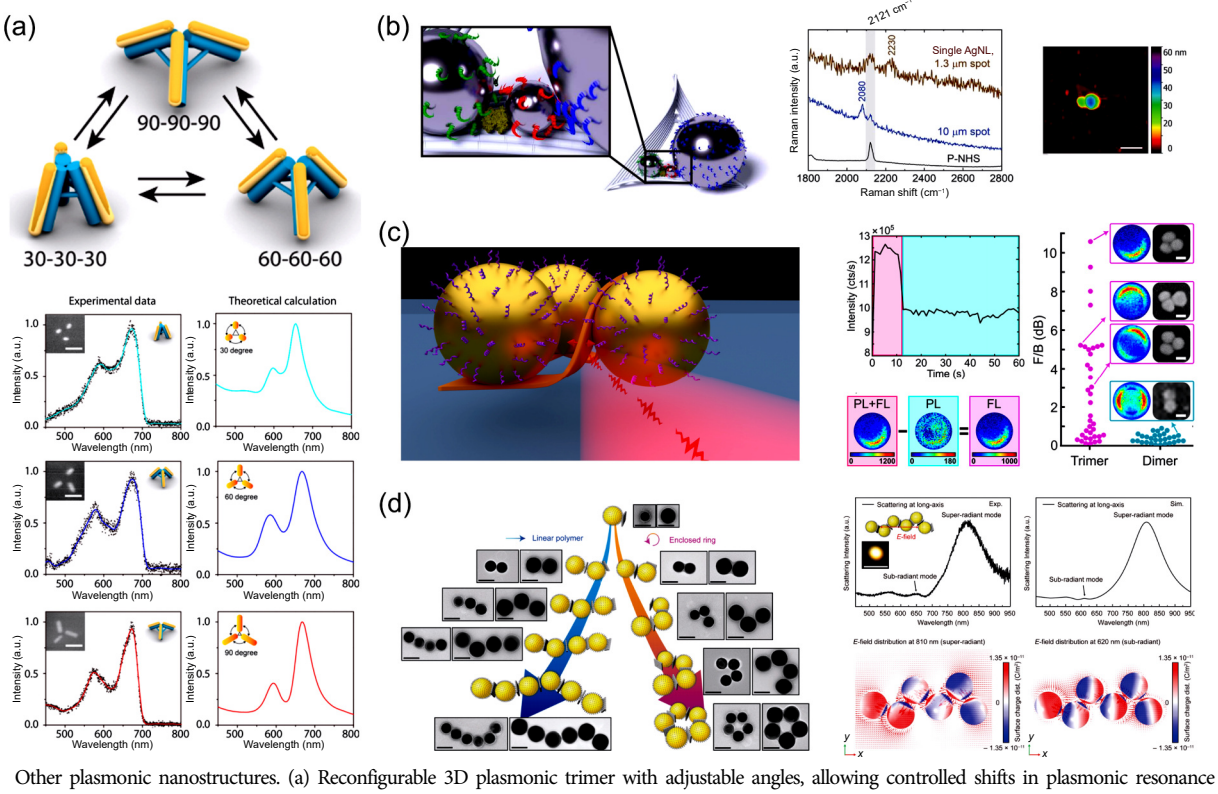

Figure 6 Other plasmonic nanostructures. (a) Reconfigurable 3D plasmonic trimer with adjustable angles, allowing controlled shifts in plasmonic resonance peaks. Reproduced with permission from Ref. [133], © American Chemical Society 2017. (b) Silver nanolenses enabled the SERS detection of a single alkyne-tagged streptavidin protein. Reproduced with permission from Ref. [134], © Wiley-VCH Verlag GmbH & Co. KGaA, Weinheim 2018. (c) Unidirectional optical meta-emitters constructed with plasmonic trimer nanoantenna and fluorescent dye. Reproduced with permission from Ref. [136], © American Chemical Society 2023. (d) Plasmonic metamolecules and chains display strong electric and unnatural magnetic resonances. Reproduced with permission from Ref. [138], © WILEY-VCH Verlag GmbH & Co. KGaA, Weinheim 2018.

transient assembly of supramolecules through the dynamics of proton concentration. These structures exhibit significant chiroptical responses, with optical properties tunable via the dynamics of chemical reaction networks, offering new insights for the development of intelligent molecular materials [135]. Beyond the aforementioned optical properties, trimers have shown promise in other applications. Huang's group investigated the unidirectional optical meta-emitters constructed through DNA origami, utilizing a plasmonic trimer nanoantenna composed of three 60 nm AuNPs and an organic fluorescent dye molecule to achieve single-molecule-level unidirectional emission. By satisfying the Kerker condition, the study achieved unidirectional emission at the emission wavelength of fluoresces, reaching a front-to-back ratio of 10.7 dB and a 23-fold fluorescence enhancement and at least five-fold increase in area efficiency compared to traditional Yagi-Uda nanoantennas (Fig. 6(c)) [136]. Numerical simulations and experimental validations demonstrated the potential of this structure in controlling light-matter interactions, highlighting its applications in brighter and faster optical wireless communication and single-photon sources for integrated photonic circuits.

DNA origami allows the construction of intricate nanoparticle assemblies, such as plasmonic metamolecules. In 2017, Liu et al. leveraged triangular DNA origami platforms to create a series of high-order heterogeneous plasmonic metamolecules. DNA-functionalized nanoparticles of various shapes were precisely positioned to form diverse heterogeneous plasmonic metamolecules, achieving complexity up to heptamers. These assemblies exhibited strong interparticle plasmonic coupling, with optical properties finely tuned by modifying the presence or absence of specific nanoparticles on the DNA origami scaffold [137]. Lee et al. employed two sides of 3D DNA origami to direct the assembly of 60 to 100 nm AuNPs into a series of plasmonic metamolecules. These structures demonstrated pronounced electric and unnatural magnetic resonances, with optical properties that could be precisely modulated by repositioning AuNPs on the DNA origami. The study provided both theoretical and experimental validation of the optical resonance characteristics of these plasmonic structures, including electromagnetic resonance, optical chirality, and exciton/electric dipole interactions. Additionally, the the oligomer chains exhibited both super-radiant and sub-radiant plasmonic resonance modes (Fig. 6(d)) [138].

Metallic nanostructures formed by metallizing DNA origami templates also exhibit plasmonic effects. Recently, our research group explored the application of DNA origami as a template for directing the shape-specific growth of metallic nanostructures. By utilizing AuNPs as connectors and DNA nanotubes as branches, we engineered AuNP-DNA origami composite nanostructures with diverse branch configurations by fine-tuning the assembly ratio of connectors to branches. Leveraging these composite structures as templates, we successfully directed the growth of various plasmonic nanostructures, including star-shaped, dumbbell-shaped, square, and hollow triangular forms. These nanostructures demonstrated LSPR effects, notably enhancing signals in SERS [139].

3.2 Periodic nanostructures

Beyond discrete nanostructures, DNA frameworks with customizable size and shape offer a powerful approach for guiding the self-assembly of nanoparticles into highly ordered formations, such as nanoparticle superlattices. Spatially organized metal nanoparticles exhibit distinct optical, magnetic, and electronic properties, driving growing interest in these nanomaterials. This section will explore three types of periodic nanoparticle assemblies: 1D, 2D, and 3D nanostructures.

3.2.1 *One-dimensional nanostructures*

Through simple assembly of double-stranded DNA, periodic 1D linear structures can be produced. For example, Gang and co-workers assembled discrete AuNRs into 1D linear structures through two DNA hybridization methods: direct hybridization and linker-induced hybridization. This mechanism was also applicable to systems involving AuNRs and AuNPs, enabling the formation of alternating linear structures. The study analyzed the evolution of the longitudinal and transverse surface plasmon bands of AuNRs using ultraviolet (UV)-visible spectroscopy [140]. In the same year, polymerase chain reaction (PCR) was introduced to assemble similar 1D linear structures (Fig. 7(a)) [141]. AuNRs modified with DNA at the sides or ends formed two types of 1D linear structures: side-by-side and end-to-end, upon entering the PCR replication system. The number of thermal cycles determined the length and complexity of the formed structures. Notably, the side-by-side structure exhibited chiral symmetry breaking, as evidenced by the bisignate nature of its CD spectrum. The experimental chiral bisignate plasmonic signals from the side-by-side structures enabled a new minimum limit for DNA detection.

DNA tiles can also serve as templates for assembling 1D linear structures. In 2004, Yan et al. demonstrated the self-assembly of controllable streptavidin conjugated AuNP linear arrays using triple DNA crossover tiles. They modified DNA triple crossover molecules with two stem loops, each containing two biotin groups, enabling the formation of three double-stranded helices via DNA self-assembly. Streptavidin was then combined with these DNA templates to create linear arrays. Additionally, AuNPs bounded to streptavidin to form linear AuNP arrays [142]. In 2009, a similar method was employed to construct 2D arrays, which eventually formed 1D tubular structures. Initially, four DX DNA tiles were used to create 2D DNA arrays, to which DNA-functionalized AuNPs were attached. Due to spatial and electrostatic repulsion, the 2D arrays spontaneously bent and rolled into 1D tubular structures. The size of the AuNPs influenced the resulting tubular structures. For instance, 5 nm AuNPs tended to form various tubular distributions, while 10 and 15 nm AuNPs favored a stacked-ring conformation. Although the study noted that the constructed structures were chiral, it did not provide specific optical characterization [143]. In contrast to earlier structures that required constructing DNA arrays before adding AuNPs, our group developed a one-step method to assemble plasmonic metamolecules (Fig. 7(b)) [144]. We designed five-strand DNA tiles to form micrometer-scale, ribbon-like DNA nanostructures, consisting of three shorter DNA strands and two longer DNA strands folded into repeating rectangular units. These five DNA strands were mixed with DNA-functionalized AuNPs or AuNRs in a single-pot process to assemble 1D linear structures. Furthermore, the 1D nanostructures demonstrated enhanced SERS signals, with intensity increasing as the size of the AuNPs increased.

Additionally, DNA origami serves as a powerful tool for constructing 1D linear arrays, offering precise control over nanoparticles to create various configurations. For instance, Wang and co-workers successfully utilized double-layer DNA origami to construct anisotropic 1D linear arrays with tailored chirality. X-shaped DNA capture strands were extended from both the upper and lower surfaces of the double-layer DNA origami to capture

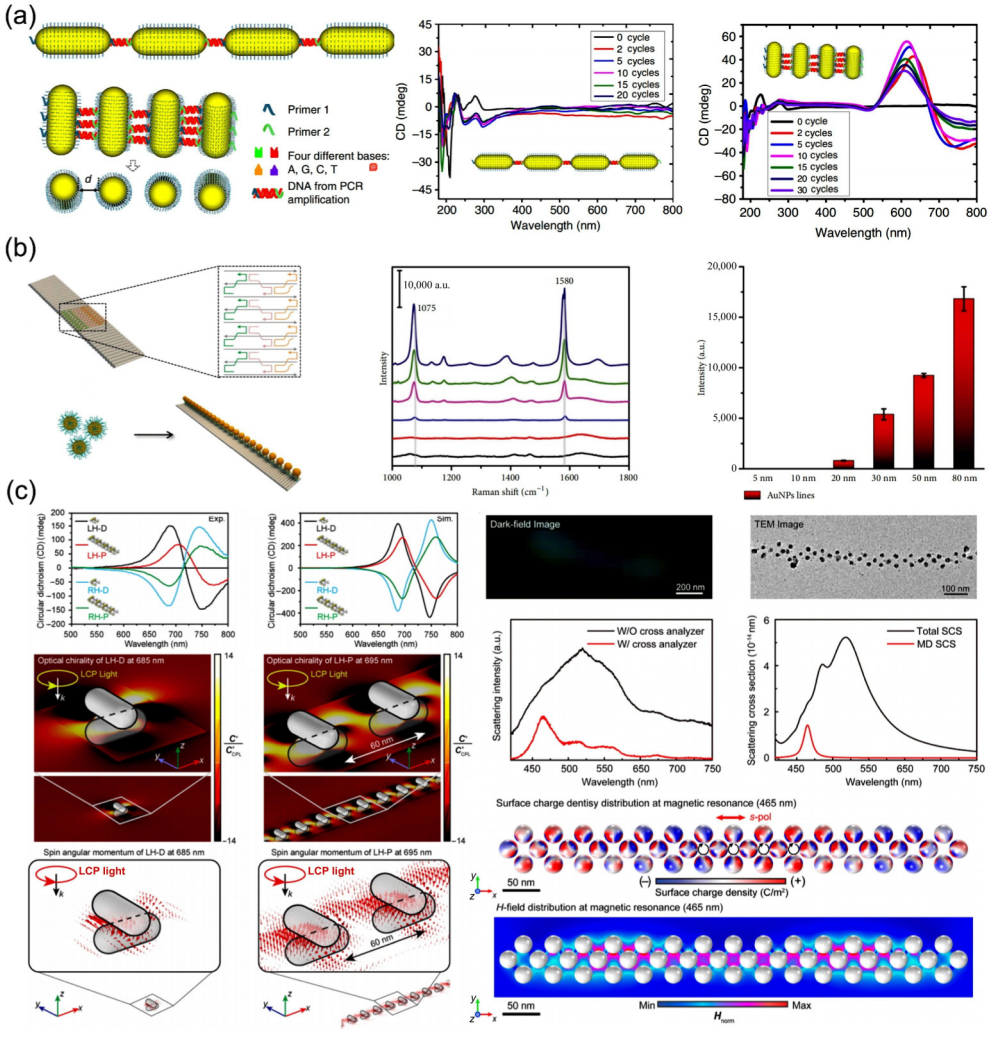

Figure 7 1D periodic nanostructures. (a) PCR assembled DNA-modified AuNRs into 1D structures, with side-by-side configuration showing chiral CD spectra. Reproduced with permission from Ref. [141], © Ma, W. et al. 2013. (b) A one-step method assembled 1D linear structures, enhancing SERS signals. Reproduced with permission from Ref. [144], © Ren, S. et al. 2019. (c) Hashtag-shaped DNA origami chains guided the formation of chiral and magnetic 1D plasmonic polymers. Reproduced with permission from Ref. [147], © American Chemical Society 2020.

DNA-functionalized AuNRs. Through the layer-by-layer assembly of AuNRs onto the double-layer DNA origami, helical superstructures of AuNRs were achieved. By adjusting the angles of the X-shaped strands, both left-handed and right-handed helical superstructures of AuNRs could be formed. The angle between adjacent AuNRs was 45°, with a spacing of 14 nm. A complete helix comprised nine AuNRs and measured approximately 220 nm in length. By varying the molar ratio of AuNRs to DNA origami, helical structures of varying lengths were obtained, thereby controlling the intensity of chiral signals [145]. Similarly, DNA origami was utilized to construct the linear superstructures of AuNPs by Gang and co-workers. They designed two multilayered "pillar" structures: pillar (3 + 3) and pillar (3 + 4). In cluster A, three identical AuNPs were assembled atop the DNA origami at sites 1, 2, and 3, leaving sites 4, 5, and 6 vacant at the bottom. Conversely, in cluster B, AuNPs were attached at the bottom sites 4, 5, and 6, leaving the upper sites vacant. The mixing of clusters A and B resulted in self-assembled ABAB pillar structures, with similar principles applied to pillar (3 + 4). These linear structures are valuable for studying the collective plasmon resonance of metal nanostructures [146]. Besides double-layer DNA origami, Ke's team designed DNA origami by orthogonal stacks of two decks, denoted as a hashtag tile and assembled as tiles to aggregate into a highly rigid 1D chain. This hashtag-shaped DNA origami chain serves as a framework allowing the robust, universal, and precise arrangement of metal nanoparticles into micron-long chiral and magnetic 1D plasmonic polymers. These structures were capable of efficiently transporting plasmonic angular momentum and magnetic surface plasmonic polaritons at deep-subwavelength scale (Fig. 7(c)) [147]. The advancement of dynamic DNA-based nanostructures is also noteworthy. This progress can be traced back to Liu and co-workers who developed 1D linear reconfigurable nanoparticle chiral superstructures capable of modulating their chiral optical properties. They designed V-shaped DNA origami and assembled AuNRs on one arm. These DNA origami monomers were layered to form helical metamolecular structures, resulting in chiral plasmonic helical superstructures of AuNRs. By employing DNA strand displacement, the angle of the V-shaped DNA origami could be altered from a tight (smaller angle) to an expanded state (larger angle). This reconfiguration led to the inversion of the plasmonic chiral signals of the AuNRs helical superstructures [148].

3.2.2 *Two-dimensional nanostructures*

In 2002, Seeman's team expanded on earlier findings by using 2D DNA crystals as templates for the self-assembly of AuNP arrays. These crystals, constructed from DNA hairpins with thiolated surfaces, enabled the formation of 2D AuNP arrays with interparticle spacing of 4 and 64 nm [149]. Later, Kiehl's team improved this method by utilizing DNA-functionalized AuNPs that hybridized with DNA scaffolds formed by DX molecules, significantly enhanced the assembly yield, though this was performed on surfaces [150]. Kiehl further refined the technique to precisely arrange multiple DNA-encoded nanocomponents, incorporating AuNPs of varying sizes to improve visualization [151]. Seeman also utilized 3D DX triangles to create 2D crystal arrays, facilitating the assembly of alternating 5 and 10 nm AuNPs [152]. Concurrently, Yan's team employed four-arm DNA branches to form periodic square structures within nanogrids, achieving precise AuNP arrays with a center-to-center spacing of 38 nm [153, 154].

The advent of DNA origami has significantly expanded types of 2D nanoparticle arrays [155]. In 2016, Gang et al. utilized DNA origami to create periodic arrays and complex structures of AuNPs (Fig. 8(a)) [156]. By using square-shaped DNA origami with cavities, they improved assembly efficiency by mitigating spatial repulsion. The design of DNA connecting strands in four directions allowed for the formation of 2D square nanoparticle arrays when these strands matched complementary strands on adjacent origami piece. Simultaneously, Ke et al. employed 3D DNA origami to assemble AuNPs into large-scale, micro-scale 2D grids. They designed various configurations of DNA origami hexagon tiles (1 × 4, 2 × 4, 4 × 2) to program the arrangement of AuNPs, leading to various plasmonic metamaterials, including 2D lattices and 3D tubular structures (Fig. 8(b)) [157]. The 2 × 4 hexagon tiles were particularly adept at forming 2D arrays with varying configurations based on the placement of AuNP. The AuNP lattices exhibited intriguing plasmonic resonance. The 30 nm_Au_2D_2 lattices displayed characteristics of electro-optical metamaterials, arising from enhanced interparticle coupling. A red shift of 15.5 nm was observed in the UV–vis absorption spectra compared to discrete 37 nm AuNPs, closing aligning well with the 14.9 nm red shift predicted by simulation data. The spatial distribution of the coupled electric field intensity between AuNPs further confirmed this capacitive coupling-enabled electric resonance within the AuNP superlattice. This lattice provided a versatile platform for the nanoengineering of artificial plasmonic metamolecules and metasurfaces. In contrast, Tian and co-workers innovatively encased AuNPs in octahedral DNA origami frames, enabling precise formation of 2D planes [158]. For other innovative approaches, Schreiber et al. assembled DNA origami structures resembling flower petals on AuNPs to control its bonding symmetry. This approach resulted in "nanoflowers" with 32 radial petals, capable of arranging AuNPs into diverse lattice structures [159]. Our group utilized AuNPs to mediate DNA nanostructures, assembling them into various discrete structures and 2D AuNP lattices [160]. These methods showcase the versatility of DNA origami in forming intricate nanoparticle arrangements.

3.2.3 *Three-dimensional nanostructures*

The 3D lattices of plasmonic nanoparticles offer a vast and intricate design space for creating novel optical materials, with the potential for excellent collective effects. However, assembling nanoparticles into these 3D lattices presents a formidable challenge. While early theoretical predictions suggested that DNA could precisely assembled inorganic nanoparticles, this concept wasn't experimentally demonstrated until 2008 by Gang's and Mirkin's groups. Gang and co-workers created a 3D lattice of AuNPs through complementary DNA base pairing, achieving a reversible assembly process by adjusting the temperature [161]. Mirkin's team used different DNA sequences to guide nanoparticles into various crystalline states. Specifically, a single DNA sequence on AuNPs results in a close-packed face-centered cubic (FCC) structure, while two different sequences formed a non-close-packed body-centered cubic (BCC) structure. These methods allow control over the dimension, crystal symmetry, and phase behavior of the superlattices, although isotropic 3D lattices are yielded [162]. Since

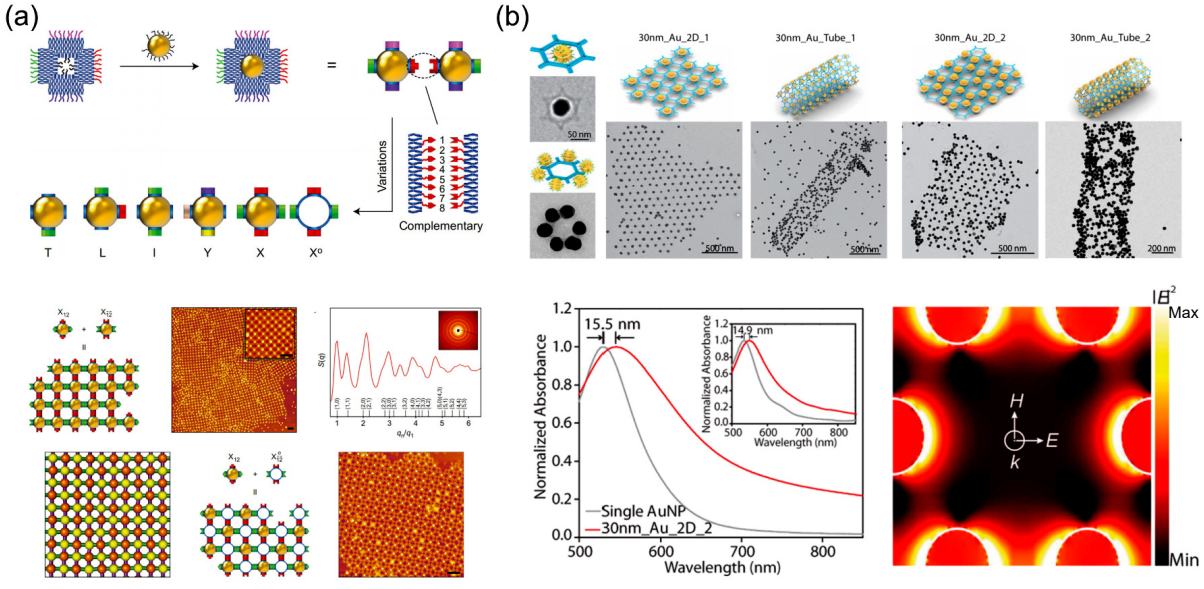

Figure 8 2D periodic nanostructures. (a) AuNPs combined with square-shaped DNA origami formed 2D nanoparticle arrays. Reproduced with permission from Ref. [156], © Springer Nature Limited 2016. (b) DNA origami hexagon tiles were programmed with AuNPs to produce various plasmonic metamaterials and their plasmonic resonance properties. Reproduced with permission from Ref. [157], © American Chemical Society 2016.

these breakthroughs, research has increasingly focused on arranging nanoparticles into specific optical 3D lattices under DNA guidance. Gang's group achieved a pioneering breakthrough by successfully assembly of 3D superlattices using DNA linkers with three distinct binding sites. These linkers served dual roles as both assembly agents and dynamically tunable structural elements. The resulting superlattices, composed of plasmonic particles (AuNPs) and chromophores (such as rhodamine) enabled researchers to modulate the distance between chromophores and the plasmonic nanoparticles within the superlattice by adjusting ionic strength. This controlled optical coupling led to a nearly threefold change in the emission rate of the chromophores, showcasing tunable optical behavior [163].

Mirkin's group has also contributed extensively to the field with several innovative studies. In 2014, they used DNA as programmable linkers to assemble AgNP superlattices, which allowed precise control over the size, spacing, and symmetry of nanoparticles in 3D space. Optical analyses via UV–Vis and optical micro-spectrophotometry revealed enhanced electric field strength at absorption and extinction maxima, particularly in forward scattering, indicating pronounced optical metallic behavior. Electrodynamic simulations corroborated the observed dielectric responses, underscoring the strong relationship between optical properties and nanoparticle spacing. Additionally, in Ag-Au binary superlattices, a Fano interference effect was noted between silver's LSPR and gold's interbond transitions, damping silver's LSPR [164]. By 2015, the team furthered these studies by assembling 3D plasmonic superlattices through DNA programming, exhibiting significant optical metallic behavior with red-shifting extinction peaks as gold volume fraction increased (i.e., decreased particle spacing), confirming the critical influence of nanoparticle spacing on optical response (Fig. 9(a)) [165]. In 2017, they advanced these assemblies by using DNA to create superlattices composed of octahedral and spherical nanoparticles, achieving BCC lattice symmetry and a macroscopic rhombic dodecahedron crystal morphology. Octahedral nanoparticles demonstrated polarization-dependent backscattering opposite to that of spherical nanoparticles, a feature stemming from their anisotropy and requiring precise nanoparticle alignment. The study identified plasmonic and photonic modes, modifiable through adjusting nanoparticle size, shape, and arrangement as well as 3D superlattice dimensions (Fig. 9(b)) [166].

Beyond simple DNA hybridization, structures such as rigid DNA grids and DNA origami have been effectively utilized to assemble nanoparticle superlattices by precisely positioning the nanoparticles. Gang's team advanced this approach by creating a series of AuNP-DNA 3D lattices using five different DNA polyhedral frameworks. By attaching single-stranded DNA at the ends of these polyhedral, which connected with DNA-functionalized AuNPs, they effectively controlled the lattice types based on the framework shapes. Additionally, they employed rigid tetrahedral DNA origami cages enabled precise assembly of AuNPs at both centers and vertices, forming two different diamond superlattices [168]. In 2020, extended their methodology, utilizing DNA origami polyhedral frames to create 3D lattices with diverse nanomaterials, including metal nanoparticles, semiconductor nanoparticles, and proteins (Fig. 9(c)) [167]. By 2020, the design was developed into 3D superconducting superlattices by first converting into silica scaffolds, which were subsequently coated with superconducting niobium, resulting in 3D arrays of Josephson junctions [169]. Inspired by Gang's work, Tian and co-workers developed a co-crystallization method using pairs of DNA origami building blocks with varying symmetry. By manipulating the ratios of regular and elongated octahedral DNA origami units, they demonstrated three

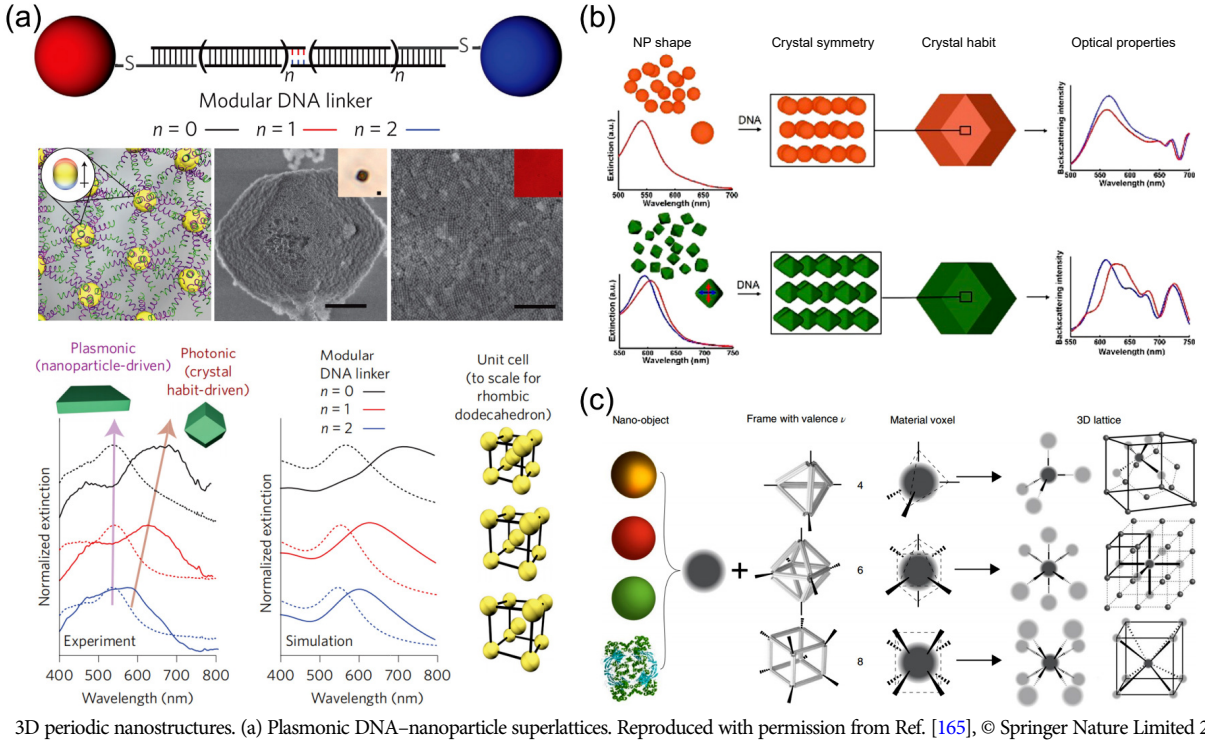

Figure 9 3D periodic nanostructures. (a) Plasmonic DNA–nanoparticle superlattices. Reproduced with permission from Ref. [165], © Springer Nature Limited 2015. (b) Polarization-dependent optical response in anisotropic nanoparticle-DNA superlattices. Reproduced with permission from Ref. [166], © American Chemical Society 2017. (c) Create 3D lattices of different types of nanomaterials. Reproduced with permission from Ref. [167], © This is a USA government work and not under copyright protection in the USA; foreign copyright protection may apply 2020.

programmable co-crystallization modes with AuNPs embedded in the octahedra [170]. In addition to the DNA polyhedral frameworks, Liedl and co-workers introduced a DNA-origami-based "tensegrity triangle" comprised of three 12-helix bundles of equal length, forming a constrained 3D symmetrical triangular structure. This configuration allows the formation of rhombic lattices with AuNPs [171].

4 Conclusions and perspectives

The development of DNA-based plasmonic nanostructures has reached a mature stage, enabling precise control over nanoparticle assembly and achieving tailored optical responses, thus significantly advancing the field of optical sensing. The programmability and structural versatility of DNA have facilitated the development of diverse plasmonic nanostructures, ranging from discrete assemblies to complex lattices. These structures exhibit remarkable optical properties, such as SERS, fluorescence enhancement, and chirality. Furthermore, due to their excellent biocompatibility and biodegradability, DNA-based plasmonic nanostructures have extensive applications in bioimaging and biosensing. For example, Xu et al. designed and synthesized a DNA origami-based plasmonic nanoantenna for the early diagnosis and intelligent treatment of acute kidney injury (AKI). They evaluated the nanoantenna's biocompatibility and safety, finding that cytotoxicity tests showed a human embryonic kidney cell survival rate above 93.3% after 24 h of high-concentration incubation, indicating low cytotoxicity. In healthy mice, blood biochemical parameters and routine blood analyses were within normal ranges, and histological examinations of major organs showed no abnormalities, demonstrating good *in vivo* biocompatibility and safety. *In vivo* distribution and metabolism studies revealed that the nanoantenna had a blood half-life of approximately 3.02 h in mice. Fluorescence imaging indicated that the nanoantenna was cleared within 24 h post-injection, with no significant accumulation observed in major organs [172].

Despite these achievements, several challenges hinder the practical application of DNA-based plasmonic nanostructures. Their synthesis often requires stringent laboratory conditions. Moreover, although DNA is biodegradable, when it combines with metal nanoparticles (such as gold or silver) to form plasmonic nanostructures, these nanoparticles may have potential toxicity. For example, the use of AgNPs in many consumer products leads to their release into aquatic environments, becoming a source of dissolved silver, which can cause toxic effects on aquatic organisms—including bacteria, algae, fish, and water fleas [173]. While DNA-based plasmonic nanostructures have significant application prospects, it is crucial to pay attention to their potential environmental impacts. High costs of DNA and the complexity of multi-step signal amplification processes further hinder large-scale application and rapid detection. Additionally, stability issues with the nanomaterials also impact the reproducibility and reliability of the results. While the construction of these nanostructures is well-established, innovation in the design of new DNA-based plasmonic nanostructures has slowed, with research increasingly focusing on applying established structures with known optical responses to biosensing, bioimaging, and biotherapy fields.

To overcome these challenges, future research should aim to develop more robust and cost-effective DNA-based systems capable of withstanding diverse environmental conditions. Interdisciplinary approaches that integrate advances in materials science, DNA nanotechnology, and molecular biology are essential for pushing the boundaries of current capabilities. By addressing these challenges, the potential of DNA-based plasmonic nanostructures can be realized, facilitating the development of high-yield, stable, and sensitive optical sensors suitable for large-scale applications. Further exploration is expected to reveal new phenomena and applications, driving innovation in optical sensing technologies. For example, Ding's group utilized DNA origami technology to combine chiral plasmonic nanostructures (assembled from AuNRs and coated with a layer of silver) with J-aggregate dye molecules (such as TDBC), constructing a chiral plexcitonic hybrid system. This hybrid system exhibited strong light-matter interactions, with observations of Rabi splitting and anti-crossing behaviors, demonstrating the possibility of achieving strong coupling in chiral optical systems [174]. This successful example indicates that by integrating DNA-based plasmonic nanostructures with other nanomaterials, it is possible to further enhance the performance of these hybrid systems.

Additionally, we envision that the integration of DNA self-assembly with top-down fabrication techniques, such as electron beam lithography, could lead to the creation of dynamic metasurfaces and metamaterials. The combination with ordered DNA lattices could pave the way for dynamic metasurfaces operating at visible wavelengths, opening new avenues for research and application. As the field progresses, it is crucial to balance the refinement of existing technologies with the pursuit of novel innovations to maintain momentum and achieve breakthroughs in DNA-based plasmonic nanostructures.

Data availability

Not applicable.

Acknowledgements

This work was supported by the National Natural Science Foundation of China (Nos. 22274081, 62288102, and 62401494), and the Natural Science Foundation of Jiangsu Province (No. BE2023839).

Declaration of competing interest

All the contributing authors report no conflict of interests in this work.

Author contribution statement

R. J. N.: Conceptualization. J. L. D.: Investigation. W. Q. H.: Supervision. B. L.: Writing – original draft. J. C.: Writing – review & editing.

Informed consent

Not applicable.

Ethics statement

Not applicable.

Use of AI statement

None.

References

[1] Kim, J. M.; Lee, C.; Lee, Y.; Lee, J.; Park, S. J.; Park, S.; Nam, J. M. Synthesis, assembly, optical properties, and sensing applications of plasmonic gap nanostructures. *Adv. Mater.* **2021**, *33*, 2006966.

[2] Zhao, J.; Xue, S.; Ji, R. R.; Li, B.; Li, J. H. Localized surface plasmon resonance for enhanced electrocatalysis. *Chem. Soc. Rev.* **2021**, *50*, 12070–12097.

[3] Pilot, R.; Signorini, R.; Durante, C.; Orian, L.; Bhamidipati, M.; Fabris, L. A review on surface-enhanced Raman scattering. *Biosensors* **2019**, *9*, 57.

[4] Hentschel, M.; Schäferling, M.; Duan, X. Y.; Giessen, H.; Liu, N. Chiral plasmonics. *Sci. Adv.* **2017**, *3*, e1602735.

[5] Ou, X. W.; Liu, Y. Q.; Zhang, M. X.; Hua, L.; Zhan, S. S. Plasmonic gold nanostructures for biosensing and bioimaging. *Microchim. Acta* **2021**, *188*, 304.

[6] Yoon, J.; Shin, M.; Lee, J. Y.; Lee, S. N.; Choi, J. H.; Choi, J. W. RNA interference (RNAi)-based plasmonic nanomaterials for cancer diagnosis and therapy. *J. Control. Release* **2022**, *342*, 228–240.

[7] Cortés, E.; Besteiro, L. V.; Alabastri, A.; Baldi, A.; Tagliabue, G.; Demetriadou, A.; Narang, P. Challenges in plasmonic catalysis. *ACS Nano* **2020**, *14*, 16202–16219.

[8] Ahmed, A.; Pelton, M.; Guest, J. R. Understanding how acoustic vibrations modulate the optical response of plasmonic metal nanoparticles. *ACS Nano* **2017**, *11*, 9360–9369.

[9] Jessen, B. S.; Gammelgaard, L.; Thomsen, M. R.; Mackenzie, D. M. A.; Thomsen, J. D.; Caridad, J. M.; Duegaard, E.; Watanabe, K.; Taniguchi, T.; Booth, T. J. et al. Lithographic band structure engineering of graphene. *Nat. Nanotechnol.* **2019**, *14*, 340–346.

[10] Oh, S.; Park, S. K.; Kim, J. H.; Cho, I.; Kim, H. J.; Park, S. Y. Patterned taping: A high-efficiency soft lithographic method for universal thin film patterning. *ACS Nano* **2016**, *10*, 3478–3485.

[11] Seeman, N. C.; Sleiman, H. F. DNA nanotechnology. *Nat. Rev. Mater.* **2018**, *3*, 17068.

[12] Jiang, Q.; Shang, Y. X.; Xie, Y. M.; Ding, B. Q. DNA origami: From molecular folding art to drug delivery technology. *Adv. Mater.* **2024**, *36*, 2301035.

[13] Nummelin, S.; Kommeri, J.; Kostiainen, M. A.; Linko, V. Evolution of structural DNA nanotechnology. *Adv. Mater.* **2018**, *30*, 1703721.

[14] Li, Y.; Pei, J.; Lu, X. H.; Jiao, Y. F.; Liu, F. S.; Wu, X. H.; Liu, J. B.; Ding, B. Q. Hierarchical assembly of super-DNA origami based on a flexible and covalent-bound branched DNA structure. *J. Am. Chem. Soc.* **2021**, *143*, 19893–19900.

[15] Wang, Y.; Yan, X. H.; Zhou, Z. Y.; Ma, N. N.; Tian, Y. Ph-induced symmetry conversion of DNA origami lattices. *Angew. Chem., Int. Ed.* **2022**, *61*, e202208290.

[16] Lan, X.; Wang, Q. B. DNA-programmed self-assembly of photonic nanoarchitectures. *NPG Asia Mater.* **2014**, *6*, e97.

[17] Liu, Q.; Song, C.; Wang, Z. G.; Li, N.; Ding, B. Q. Precise organization of metal nanoparticles on DNA origami template. *Methods* **2014**, *67*, 205–214.

[18] Liu, N.; Liedl, T. DNA-assembled advanced plasmonic architectures. *Chem. Rev.* **2018**, *118*, 3032–3053.

[19] Zhu, R.; Li, J.; Lin, L. S.; Song, J. B.; Yang, H. H. Emerging plasmonic assemblies triggered by DNA for biomedical applications. *Adv. Funct. Mater.* **2021**, *31*, 2005709.

[20] Seeman, N. C. Nucleic acid junctions and lattices. *J. Theor. Biol.* **1982**, *99*, 237–247.

[21] Fu, T. J.; Seeman, N. C. DNA double-crossover molecules. *Biochemistry* **1993**, *32*, 3211–3220.

[22] Winfree, E.; Liu, F. R.; Wenzler, L. A.; Seeman, N. C. Design and self-assembly of two-dimensional DNA crystals. *Nature* **1998**, *394*, 539–544.

[23] Mao, C. D.; Sun, W. Q.; Shen, Z. Y.; Seeman, N. C. A nanomechanical device based on the B–Z transition of DNA. *Nature* **1999**, *397*, 144–146.

[24] LaBean, T. H.; Yan, H.; Kopatsch, J.; Liu, F. R.; Winfree, E.; Reif, J. H.; Seeman, N. C. Construction, analysis, ligation, and self-assembly of DNA triple crossover complexes. *J. Am. Chem. Soc.* **2000**, *122*, 1848–1860.

[25] Maiti, P. K.; Pascal, T. A.; Vaidehi, N.; Goddard III, W. A. The stability of seeman JX DNA topoisomers of paranemic crossover (PX) molecules as a function of crossover number. *Nucleic Acids Res.* **2004**, *32*, 6047–6056.

[26] Shen, Z. Y.; Yan, H.; Wang, T.; Seeman, N. C. Paranemic crossover DNA: A generalized holliday structure with applications in nanotechnology. *J. Am. Chem. Soc.* **2004**, *126*, 1666–1674.

[27] Majumder, U.; Rangnekar, A.; Gothelf, K. V.; Reif, J. H.; LaBean, T. H. Design and construction of double-decker tile as a route to three-dimensional periodic assembly of DNA. *J. Am. Chem. Soc.* **2011**, *133*, 3843–3845.

[28] Shih, W. M.; Quispe, J. D.; Joyce, G. F. A 1.7-kilobase single-stranded DNA that folds into a nanoscale octahedron. *Nature* **2004**, *427*, 618–621.

[29] Rothemund, P. W. K. Folding DNA to create nanoscale shapes and patterns. *Nature* **2006**, *440*, 297–302.

[30] Douglas, S. M.; Dietz, H.; Liedl, T.; Högberg, B.; Graf, F.; Shih, W. M. Self-assembly of DNA into nanoscale three-dimensional shapes. *Nature* **2009**, *459*, 414–418.

[31] Yang, Y.; Han, D. R.; Nangreave, J.; Liu, Y.; Yan, H. DNA origami with double-stranded DNA as a unified scaffold. *ACS Nano* **2012**, *6*, 8209–8215.

[32] Hong, F.; Zhang, F.; Liu, Y.; Yan, H. DNA origami: Scaffolds for creating higher order structures. *Chem. Rev.* **2017**, *117*, 12584–12640.

[33] Xing, Y. Z.; Dorey, A.; Jayasinghe, L.; Howorka, S. Highly shape- and size-tunable membrane nanopores made with DNA. *Nat. Nanotechnol.* **2022**, *17*, 708–713.

[34] Rossi-Gendron, C.; El Fakih, F.; Bourdon, L.; Nakazawa, K.; Finkel, J.; Triomphe, N.; Chocron, L.; Endo, M.; Sugiyama, H.; Bellot, G. et al. Isothermal self-assembly of multicomponent and evolutive DNA nanostructures. *Nat. Nanotechnol.* **2023**, *18*, 1311–1318.

[35] Ji, W.; Xiong, X. W.; Cao, M. Y.; Zhu, Y.; Li, L.; Wang, F.; Fan, C. H.; Pei, H. Encoding signal propagation on topology-programmed DNA origami. *Nat. Chem.* **2024**, *16*, 1408–1417.

[36] Andersen, E. S.; Dong, M. D.; Nielsen, M. M.; Jahn, K.; Lind-Thomsen, A.; Mamdouh, W.; Gothelf, K. V.; Besenbacher, F.; Kjems, J. DNA origami design of dolphin-shaped structures with flexible tails. *ACS Nano* **2008**, *2*, 1213–1218.

[37] Bohlin, J.; Matthies, M.; Poppleton, E.; Procyk, J.; Mallya, A.; Yan, H.; Šulc, P. Design and simulation of DNA, RNA and hybrid protein-nucleic acid nanostructures with oxView. *Nat. Protoc.* **2022**, *17*, 1762–1788.

[38] Ke, Y. G.; Ong, L. L.; Shih, W. M.; Yin, P. Three-dimensional structures self-assembled from DNA bricks. *Science* **2012**, *338*, 1177–1183.

[39] Wei, B.; Dai, M. J.; Yin, P. Complex shapes self-assembled from single-stranded DNA tiles. *Nature* **2012**, *485*, 623–626.

[40] Deng, J.; Walther, A. Autonomous DNA nanostructures instructed by hierarchically concatenated chemical reaction networks. *Nat. Commun.* **2021**, *12*, 5132.

[41] Chen, R.; Feng, S.; Ren, J. L.; Kang, H.; Yang, Y. F.; Xia, N. N.; Fang, F.; Wei, B. Enzymatic assembly of DNA nanostructures and fragments with sequence overlaps. *J. Am. Chem. Soc.* **2023**, *145*, 9176–9181.

[42] Yang, Q.; Chang, X.; Lee, J. Y.; Saji, M.; Zhang, F. DNA T-shaped crossover tiles for 2D tessellation and nanoring reconfiguration. *Nat. Commun.* **2023**, *14*, 7675.

[43] Douglas, S. M.; Bachelet, I.; Church, G. M. A logic-gated nanorobot

for targeted transport of molecular payloads. *Science* **2012**, *335*, 831–834.
[44] Yurke, B.; Turberfield, A. J.; Mills, A. P. Jr. ; Simmel, F. C.; Neumann, J. L. A DNA-fuelled molecular machine made of DNA. *Nature* **2000**, *406*, 605–608.
[45] Li, Y. L.; Tian, C.; Liu, Z. Y.; Jiang, W.; Mao, C. D. Structural transformation: Assembly of an otherwise inaccessible DNA nanocage. *Angew. Chem., Int. Ed.* **2015**, *54*, 5990–5993.
[46] Gerling, T.; Wagenbauer, K. F.; Neuner, A. M.; Dietz, H. Dynamic DNA devices and assemblies formed by shape-complementary, non-base pairing 3D components. *Science* **2015**, *347*, 1446–1452.
[47] Liu, S. L.; Jiang, Q.; Zhao, X.; Zhao, R. F.; Wang, Y. N.; Wang, Y. M.; Liu, J. B.; Shang, Y. X.; Zhao, S.; Wu, T. T. et al. A DNA nanodevice-based vaccine for cancer immunotherapy. *Nat. Mater.* **2021**, *20*, 421–430.
[48] Yin, J.; Wang, S. Y.; Wang, J. H.; Zhang, Y. W.; Fan, C. H.; Chao, J.; Gao, Y.; Wang, L. H. An intelligent DNA nanodevice for precision thrombolysis. *Nat. Mater.* **2024**, *23*, 854–862.
[49] Kim, M.; Lee, C.; Jeon, K.; Lee, J. Y.; Kim, Y. J.; Lee, J. G.; Kim, H.; Cho, M.; Kim, D. N. Harnessing a paper-folding mechanism for reconfigurable DNA origami. *Nature* **2023**, *619*, 78–86.
[50] Zolfaghari, A.; Chen, T. T.; Yi, A. Y. Additive manufacturing of precision optics at micro and nanoscale. *Int. J. Extrem. Manuf.* **2019**, *1*, 012005.
[51] Zeng, S.; Liu, X. S.; Kafuti, Y. S.; Kim, H.; Wang, J. Y.; Peng, X. J.; Li, H. D.; Yoon, J. Fluorescent dyes based on rhodamine derivatives for bioimaging and therapeutics: Recent progress, challenges, and prospects. *Chem. Soc. Rev.* **2023**, *52*, 5607–5651.
[52] Liu, D.; Shi, L.; Dai, Q. B.; Lin, X. N.; Mehmood, R.; Gu, Z.; Dai, L. M. Functionalization of carbon nanotubes for multifunctional applications. *Trends Chem.* **2024**, *6*, 186–210.
[53] Mohanty, A. K.; Vivekanandhan, S.; Das, O.; Romero Millán, L. M.; Klinghoffer, N. B.; Nzihou, A.; Misra, M. Biocarbon materials. *Nat. Rev. Methods Primers* **2024**, *4*, 19.
[54] Alivisatos, A. P.; Johnsson, K. P.; Peng, X. G.; Wilson, T. E.; Loweth, C. J.; Bruchez, M. P. Jr. ; Schultz, P. G. Organization of 'nanocrystal molecules' using DNA. *Nature* **1996**, *382*, 609–611.
[55] Wang, H. Q.; Li, Y. L.; Liu, M.; Gong, M.; Deng, Z. X. Overcoming the coupling dilemma in DNA-programmable nanoparticle assemblies by "Ag^+ soldering". *Small* **2015**, *11*, 2247–2251.
[56] Chen, J. I. L.; Chen, Y.; Ginger, D. S. Plasmonic nanoparticle dimers for optical sensing of DNA in complex media. *J. Am. Chem. Soc.* **2010**, *132*, 9600–9601.
[57] Lan, X.; Chen, Z.; Dai, G. L.; Lu, X. X.; Ni, W. H.; Wang, Q. B. Bifacial DNA origami-directed discrete, three-dimensional, anisotropic plasmonic nanoarchitectures with tailored optical chirality. *J. Am. Chem. Soc.* **2013**, *135*, 11441–11444.
[58] Tang, L. J.; Li, S.; Han, F.; Liu, L. Q.; Xu, L. G.; Ma, W.; Kuang, H.; Li, A. K.; Wang, L. B.; Xu, C. L. SERS-active Au@Ag nanorod dimers for ultrasensitive dopamine detection. *Biosens. Bioelectron.* **2015**, *71*, 7–12.
[59] Tang, L. J.; Li, S.; Xu, L. G.; Ma, W.; Kuang, H.; Wang, L. B.; Xu, C. L. Chirality-based Au@Ag nanorod dimers sensor for ultrasensitive PSA detection. *ACS Appl. Mater. Inter.* **2015**, *7*, 12708–12712.
[60] Simoncelli, S.; Roller, E. M.; Urban, P.; Schreiber, R.; Turberfield, A. J.; Liedl, T.; Lohmüller, T. Quantitative single-molecule surface-enhanced Raman scattering by optothermal tuning of DNA origami-assembled plasmonic nanoantennas. *ACS Nano* **2016**, *10*, 9809–9815.
[61] Schuknecht, F.; Kołątaj, K.; Steinberger, M.; Liedl, T.; Lohmueller, T. Accessible hotspots for single-protein SERS in DNA-origami assembled gold nanorod dimers with tip-to-tip alignment. *Nat. Commun.* **2023**, *14*, 7192.
[62] Kanehira, Y.; Kogikoski, S. Jr. ; Titov, E.; Tapio, K.; Mostafa, A.; Bald, I. Watching a single enzyme at work using single-molecule surface-enhanced Raman scattering and DNA origami-based plasmonic antennas. *ACS Nano* **2024**, *18*, 20191–20200.
[63] Liu, Z.; Wang, Z. H.; Guckel, J.; Akbarian, Z.; Seifert, T. J.; Park, D.; Schlickum, U.; Stosch, R.; Etzkorn, M. Controlling nanoparticle distance by on-surface DNA-origami folding. *Small* **2024**, *20*, 2310955.
[64] Mostafa, A.; Kanehira, Y.; Tapio, K.; Bald, I. From bulk to single molecules: Surface-enhanced Raman scattering of cytochrome C using plasmonic DNA origami nanoantennas. *Nano Lett.* **2024**, *24*, 6916–6923.
[65] Sharma, M.; Kaur, C.; Singhmar, P.; Rai, S.; Sen, T. DNA origami-templated gold nanorod dimer nanoantennas: Enabling addressable optical hotspots for single cancer biomarker SERS detection. *Nanoscale* **2024**, *16*, 15128–15140.
[66] Wu, L. T.; Tanwar, S.; Kaur, G.; Date, S.; Goel, L.; Chatterjee, A.; McGuiggan, P.; Barman, I. DNA origami-engineered plasmonic nanoprobes for targeted cancer imaging. *Adv. Funct. Mater.* **2024**, *34*, 2309929.
[67] Acuna, G. P.; Möller, F. M.; Holzmeister, P.; Beater, S.; Lalkens, B.; Tinnefeld, P. Fluorescence enhancement at docking sites of DNA-directed self-assembled nanoantennas. *Science* **2012**, *338*, 506–510.
[68] Jiang, Q.; Liu, Q.; Shi, Y. F.; Wang, Z. G.; Zhan, P. F.; Liu, J. B.; Liu, C.; Wang, H.; Shi, X. H.; Zhang, L. et al. Stimulus-responsive plasmonic chiral signals of gold nanorods organized on DNA origami. *Nano Lett.* **2017**, *17*, 7125–7130.
[69] Xin, L.; Zhou, C.; Duan, X. Y.; Liu, N. A rotary plasmonic nanoclock. *Nat. Commun.* **2019**, *10*, 5394.
[70] Liu, Y.; Ge, H.; Wang, Y. Q.; Tang, L. L.; Pei, Y. F.; Fan, S. S.; Song, Y. X.; Zhang, C.; Song, J. Multistep transformations of DNA origami domino array via mechanical forces. *Small Struct.* **2023**, *4*, 2200167.
[71] Liu, F. S.; Li, N.; Shang, Y. X.; Wang, Y. M.; Liu, Q.; Ma, Z. T.; Jiang, Q.; Ding, B. Q. A DNA-based plasmonic nanodevice for cascade signal amplification. *Angewandte Chemie* **2022**, *61*, e202114706.
[72] Song, X. J.; Wang, Y. L.; Hao, Y.; Zhu, Q. Q.; Li, Y. J.; Song, L.; Deng, Z. X. Sub-1.5 nm-gapped heterodimeric plasmonic nanomolecules. *Chem. Sci.* **2022**, *13*, 4788–4793.
[73] Lim, D. K.; Jeon, K. S.; Kim, H. M.; Nam, J. M.; Suh, Y. D. Nanogap-engineerable Raman-active nanodumbbells for single-molecule detection. *Nat. Mater.* **2010**, *9*, 60–67.
[74] Hao, C. L.; Xu, L. G.; Ma, W.; Wang, L. B.; Kuang, H.; Xu, C. L. Assembled plasmonic asymmetric heterodimers with tailorable chiroptical response. *Small* **2014**, *10*, 1805–1812.
[75] Weller, L.; Thacker, V. V.; Herrmann, L. O.; Hemmig, E. A.; Lombardi, A.; Keyser, U. F.; Baumberg, J. J. Gap-dependent coupling of Ag–Au nanoparticle heterodimers using DNA origami-based self-assembly. *ACS Photonics* **2016**, *3*, 1589–1595.
[76] Kanehira, Y.; Tapio, K.; Wegner, G.; Kogikoski, S. Jr. ; Rüstig, S.; Prietzel, C.; Busch, K.; Bald, I. The effect of nanoparticle composition on the surface-enhanced Raman scattering performance of plasmonic DNA origami nanoantennas. *ACS Nano* **2023**, *17*, 21227–21239.
[77] Yu, Y.; Lei, Y. X.; Dong, Q.; Li, Y. L. Functionalization of tile-based DNA nanocages with gold nanoparticles (AuNPs) to form AuNP cluster-DNA cage hybrids. *ChemNanoMat* **2020**, *6*, 1175–1178.
[78] Chen, X. L.; Ding, L. J.; Wang, Y.; Gao, Z. S.; Li, J.; Liu, X. G.; Wang, L. H.; Zhu, Y.; Fan, C. H.; Jia, S. S. et al. Welded gold nanoparticle assemblies defined plasmonic coupling. *Nano Lett.* **2024**, *24*, 8956–8963.
[79] Mastroianni, A. J.; Claridge, S. A.; Alivisatos, A. P. Pyramidal and chiral groupings of gold nanocrystals assembled using DNA scaffolds. *J. Am. Chem. Soc.* **2009**, *131*, 8455–8459.
[80] Yan, W. J.; Xu, L. G.; Xu, C. L.; Ma, W.; Kuang, H.; Wang, L. B.; Kotov, N. A. Self-assembly of chiral nanoparticle pyramids with

strong *R/S* optical activity. *J. Am. Chem. Soc.* **2012**, *134*, 15114–15121.

[81] Sun, M. Z.; Hao, T. T.; Li, X. Y.; Qu, A. H.; Xu, L. G.; Hao, C. L.; Xu, C. L.; Kuang, H. Direct observation of selective autophagy induction in cells and tissues by self-assembled chiral nanodevice. *Nat. Commun.* **2018**, *9*, 4494.

[82] Xu, L. G.; Yan, W. J.; Ma, W.; Kuang, H.; Wu, X. L.; Liu, L.; Zhao, Y.; Wang, L. B.; Xu, C. L. SERS encoded silver pyramids for attomolar detection of multiplexed disease biomarkers. *Adv. Mater.* **2015**, *27*, 1706–1711.

[83] Shen, X. B.; Asenjo-Garcia, A.; Liu, Q.; Jiang, Q.; de Abajo, F. J. G.; Liu, N.; Ding, B. Q. Three-dimensional plasmonic chiral tetramers assembled by DNA origami. *Nano Lett.* **2013**, *13*, 2128–2133.

[84] Pilo-Pais, M.; Watson, A.; Demers, S.; LaBean, T. H.; Finkelstein, G. Surface-enhanced Raman scattering plasmonic enhancement using DNA origami-based complex metallic nanostructures. *Nano Lett.* **2014**, *14*, 2099–2104.

[85] Roller, E. M.; Khorashad, L. K.; Fedoruk, M.; Schreiber, R.; Govorov, A. O.; Liedl, T. DNA-assembled nanoparticle rings exhibit electric and magnetic resonances at visible frequencies. *Nano Lett.* **2015**, *15*, 1368–1373.

[86] Chao, J.; Zhang, Y. N.; Zhu, D.; Liu, B.; Cui, C. J.; Su, S.; Fan, C. H.; Wang, L. H. Hetero-assembly of gold nanoparticles on a DNA origami template. *Sci. China Chem.* **2016**, *59*, 730–734.

[87] Zhao, M. Z.; Wang, X.; Ren, S. K.; Xing, Y. K.; Wang, J.; Teng, N.; Zhao, D. X.; Liu, W.; Zhu, D.; Su, S. et al. Cavity-type DNA origami-based plasmonic nanostructures for Raman enhancement. *ACS Appl. Mater. Interfaces* **2017**, *9*, 21942–21948.

[88] Fang, W. N.; Jia, S. S.; Chao, J.; Wang, L. Q.; Duan, X. Y.; Liu, H. J.; Li, Q.; Zuo, X. L.; Wang, L. H.; Wang, L. H. et al. Quantizing single-molecule surface-enhanced Raman scattering with DNA origami metamolecules. *Sci. Adv.* **2019**, *5*, eaau4506.

[89] Mucic, R. C.; Storhoff, J. J.; Mirkin, C. A.; Letsinger, R. L. DNA-directed synthesis of binary nanoparticle network materials. *J. Am. Chem. Soc.* **1998**, *120*, 12674–12675.

[90] Ma, W.; Fu, P.; Sun, M. Z.; Xu, L. G.; Kuang, H.; Xu, C. L. Dual quantification of MicroRNAs and telomerase in living cells. *J. Am. Chem. Soc.* **2017**, *139*, 11752–11759.

[91] Qu, A. H.; Xu, L. G.; Sun, M. Z.; Liu, L. Q.; Kuang, H.; Xu, C. L. Photoactive hybrid AuNR-Pt@Ag_2S core-satellite nanostructures for near-infrared quantitive cell imaging. *Adv. Funct. Mater.* **2017**, *27*, 1703408.

[92] He, M. Q.; Chen, S.; Yao, K.; Wang, K.; Yu, Y. L.; Wang, J. H. Oriented assembly of gold nanoparticles with freezing-driven surface DNA manipulation and its application in SERS-based MicroRNA assay. *Small Methods* **2019**, *3*, 1900017.

[93] Feng, N.; Zhang, L.; Shen, J. J.; Hu, Y. L.; Wu, W. B.; Kouadio Fodjo, E.; Chen, S. F.; Huang, W.; Wang, L. H. SERS molecular-ruler based DNA aptamer single-molecule and its application to multi-level optical storage. *Chem. Eng. J.* **2022**, *433*, 133666.

[94] Maye, M. M.; Nykypanchuk, D.; Cuisinier, M.; van der Lelie, D.; Gang, O. Stepwise surface encoding for high-throughput assembly of nanoclusters. *Nat. Mater.* **2009**, *8*, 388–391.

[95] Li, L. L.; Wu, P. W.; Hwang, K.; Lu, Y. An exceptionally simple strategy for DNA-functionalized up-conversion nanoparticles as biocompatible agents for nanoassembly, DNA delivery, and imaging. *J. Am. Chem. Soc.* **2013**, *135*, 2411–2414.

[96] Xu, L. G.; Hao, C. L.; Yin, H. H.; Liu, L. Q.; Ma, W.; Wang, L. B.; Kuang, H.; Xu, C. L. Plasmonic core-satellites nanostructures with high chirality and bioproperty. *J. Phys. Chem. Lett.* **2013**, *4*, 2379–2384.

[97] Zhang, T. T.; Li, H.; Hou, S. W.; Dong, Y. Q.; Pang, G. S.; Zhang, Y. W. Construction of plasmonic core-satellite nanostructures on substrates based on DNA-directed self-assembly as a sensitive and reproducible biosensor. *ACS Appl. Mater. Interfaces* **2015**, *7*, 27131–27139.

[98] Li, M. X.; Xu, C. H.; Zhang, N.; Qian, G. S.; Zhao, W.; Xu, J. J.; Chen, H. Y. Exploration of the kinetics of toehold-mediated strand displacement via plasmon rulers. *ACS Nano* **2018**, *12*, 3341–3350.

[99] Liu, C. H.; Chen, C.; Li, S. Z.; Dong, H. F.; Dai, W. H.; Xu, T. L.; Liu, Y.; Yang, F.; Zhang, X. J. Target-triggered catalytic hairpin assembly-induced core-satellite nanostructures for high-sensitive "off-to-on" SERS detection of intracellular MicroRNA. *Anal. Chem.* **2018**, *90*, 10591–10599.

[100] Qu, A. H.; Sun, M. Z.; Xu, L. G.; Hao, C. L.; Wu, X. L.; Xu, C. L.; Kotov, N. A.; Kuang, H. Quantitative zeptomolar imaging of miRNA cancer markers with nanoparticle assemblies. *Proc. Natl. Acad. Sci. USA* **2019**, *116*, 3391–3400.

[101] Meng, D.; Ma, W.; Wu, X. L.; Xu, C. L.; Kuang, H. DNA-driven two-layer core-satellite gold nanostructures for ultrasensitive MicroRNA detection in living cells. *Small* **2020**, *16*, 2000003.

[102] Le, N. H.; Cathcart, N.; Kitaev, V.; Chen, J. I. L. Core-satellite assembly of gold nanoshells on solid gold nanoparticles for a color coding plasmonic nanosensor. *Analyst* **2022**, *147*, 155–164.

[103] Zhang, D. D.; Wang, K.; Wei, W.; Liu, Y.; Liu, S. Q. Multifunctional plasmonic core-satellites nanoprobe for cancer diagnosis and therapy based on a cascade reaction induced by microrna. *Anal. Chem.* **2021**, *93*, 9521–9530.

[104] Trinh, H. D.; Yoon, S. Silica-encapsulated core-satellite gold nanoparticle assemblies as stable, sensitive, and multiplex surface-enhanced Raman scattering probes. *ACS Appl. Nano Mater.* **2022**, *5*, 5087–5095.

[105] Tan, Y.; Zhou, J. X.; Xing, X. T.; Wang, J. R.; Huang, J. K.; Liu, H. Y.; Chen, J. J.; Dong, M. J.; Xiang, Q.; Dong, H. F. et al. DNA assembly of plasmonic nanostructures enables *in vivo* SERS-based MicroRNA detection and tumor photoacoustic imaging. *Anal. Chem.* **2023**, *95*, 11236–11242.

[106] Jaitpal, S.; Ng, K. W.; Juan, A. M. S.; Martinez, C.; Phillips, C.; Tripathy, S.; Mabbott, S. DNA-directed formation of plasmonic core-satellite nanostructures for quantification of hepatitis C viral RNA. *Chem. Sci.* **2024**, *15*, 8112–8126.

[107] Xu, L. G.; Kuang, H.; Xu, C. L.; Ma, W.; Wang, L. B.; Kotov, N. A. Regiospecific plasmonic assemblies for *in situ* Raman spectroscopy in live cells. *J. Am. Chem. Soc.* **2012**, *134*, 1699–1709.

[108] Zhang, Y. N.; Chao, J.; Liu, H. J.; Wang, F.; Su, S.; Liu, B.; Zhang, L.; Shi, J. Y.; Wang, L. H.; Huang, W. et al. Transfer of two-dimensional oligonucleotide patterns onto stereocontrolled plasmonic nanostructures through DNA-origami-based nanoimprinting lithography. *Angew. Chem., Int. Ed.* **2016**, *55*, 8036–8040.

[109] Liu, B.; Song, C. Y.; Zhu, D.; Wang, X.; Zhao, M. Z.; Yang, Y. J.; Zhang, Y. N.; Su, S.; Shi, J. Y.; Chao, J. et al. DNA-origami-based assembly of anisotropic plasmonic gold nanostructures. *Small* **2017**, *13*, 1603991.

[110] Niu, R. J.; Song, C. Y.; Gao, F.; Fang, W. N.; Jiang, X. Y.; Ren, S. K.; Zhu, D.; Su, S.; Chao, J.; Chen, S. F. et al. DNA origami-based nanoprinting for the assembly of plasmonic nanostructures with single-molecule surface-enhanced Raman scattering. *Angew. Chem., Int. Ed.* **2021**, *60*, 11695–11701.

[111] Edwardson, T. G. W.; Lau, K. L.; Bousmail, D.; Serpell, C. J.; Sleiman, H. F. Transfer of molecular recognition information from DNA nanostructures to gold nanoparticles. *Nat. Chem.* **2016**, *8*, 162–170.

[112] Xie, N. L.; Liu, S. Y.; Fang, H. M.; Yang, Y. J.; Quan, K.; Li, J.; Yang, X. H.; Wang, K. M.; Huang, J. Three-dimensional molecular transfer from DNA nanocages to inner gold nanoparticle surfaces. *ACS Nano* **2019**, *13*, 4174–4182.

[113] Kuzyk, A.; Schreiber, R.; Fan, Z. Y.; Pardatscher, G.; Roller, E. M.; Högele, A.; Simmel, F. C.; Govorov, A. O.; Liedl, T. DNA-based self-assembly of chiral plasmonic nanostructures with tailored optical response. *Nature* **2012**, *483*, 311–314.

[114] Shen, X. B.; Song, C.; Wang, J. Y.; Shi, D. W.; Wang, Z. G.; Liu, N.;

Ding, B. Q. Rolling up gold nanoparticle-dressed DNA origami into three-dimensional plasmonic chiral nanostructures. *J. Am. Chem. Soc.* **2012**, *134*, 146–149.

[115] Martens, K.; Funck, T.; Kempter, S.; Roller, E. M.; Liedl, T.; Blaschke, B. M.; Knecht, P.; Garrido, J. A.; Zhang, B. R.; Kitzerow, H. Alignment and graphene-assisted decoration of lyotropic chromonic liquid crystals containing DNA origami nanostructures. *Small* **2016**, *12*, 1658–1666.

[116] Shen, C. Q.; Lan, X.; Zhu, C. G.; Zhang, W.; Wang, L. Y.; Wang, Q. B. Spiral patterning of Au nanoparticles on Au nanorod surface to form chiral AuNR@AuNP helical superstructures templated by DNA origami. *Adv. Mater.* **2017**, *29*, 1606533.

[117] Benn, F.; Haley, N. E. C.; Lucas, A. E.; Silvester, E.; Helmi, S.; Schreiber, R.; Bath, J.; Turberfield, A. J. Chiral DNA origami nanotubes with well-defined and addressable inside and outside surfaces. *Angew. Chem., Int. Ed.* **2018**, *57*, 7687–7690.

[118] Golla, M.; Albert, S. K.; Atchimnaidu, S.; Perumal, D.; Krishnan, N.; Varghese, R. DNA-decorated, helically twisted nanoribbons: A scaffold for the fabrication of one-dimensional, chiral, plasmonic nanostructures. *Angew. Chem., Int. Ed.* **2019**, *58*, 3865–3869.

[119] Ma, L.; Liu, Y.; Han, C.; Movsesyan, A.; Li, P. H.; Li, H. C.; Tang, P.; Yuan, Y. Q.; Jiang, S. X.; Ni, W. H. et al. DNA-assembled chiral satellite-core nanoparticle superstructures: Two-state chiral interactions from dynamic and static conformations. *Nano Lett.* **2022**, *22*, 4784–4791.

[120] Martens, K.; Funck, T.; Santiago, E. Y.; Govorov, A. O.; Burger, S.; Liedl, T. Onset of chirality in plasmonic meta-molecules and dielectric coupling. *ACS Nano* **2022**, *16*, 16143–16149.

[121] Peil, A.; Zhan, P. F.; Duan, X. Y.; Krahne, R.; Garoli, D.; Liz-Marzán, L. M.; Liu, N. Transformable plasmonic helix with swinging gold nanoparticles. *Angew. Chem., Int. Ed.* **2023**, *62*, e202213992.

[122] Cecconello, A.; Cencini, A.; Rilievo, G.; Tonolo, F.; Litti, L.; Vianello, F.; Willner, I.; Magro, M. Chiroplasmonic DNA scaffolded "fusilli" structures. *Nano Lett.* **2024**, *24*, 5944–5951.

[123] Schreiber, R.; Luong, N.; Fan, Z. Y.; Kuzyk, A.; Nickels, P. C.; Zhang, T.; Smith, D. M.; Yurke, B.; Kuang, W.; Govorov, A. O. et al. Chiral plasmonic DNA nanostructures with switchable circular dichroism. *Nat. Commun.* **2013**, *4*, 2948.

[124] Cecconello, A.; Kahn, J. S.; Lu, C. H.; Khosravi Khorashad, L.; Govorov, A. O.; Willner, I. DNA scaffolds for the dictated assembly of left-/right-handed plasmonic Au NP helices with programmed chiro-optical properties. *J. Am. Chem. Soc.* **2016**, *138*, 9895–9901.

[125] Urban, M. J.; Dutta, P. K.; Wang, P. F.; Duan, X. Y.; Shen, X. B.; Ding, B. Q.; Ke, Y. G.; Liu, N. Plasmonic toroidal metamolecules assembled by DNA origami. *J. Am. Chem. Soc.* **2016**, *138*, 5495–5498.

[126] Wang, M.; Dong, J. Y.; Zhou, C.; Xie, H.; Ni, W. H.; Wang, S.; Jin, H. L.; Wang, Q. B. Reconfigurable plasmonic diastereomers assembled by DNA origami. *ACS Nano* **2019**, *13*, 13702–13708.

[127] Kim, T.; Lee, C.; Lee, J. Y.; Kim, D. N. Controlling chiroptical responses via chemo-mechanical deformation of DNA origami structures. *ACS Nano* **2024**, *18*, 3414–3423.

[128] Zhang, C.; Li, X.; Tian, C.; Yu, G. M.; Li, Y. L.; Jiang, W.; Mao, C. D. DNA nanocages swallow gold nanoparticles (AuNPs) to form AuNP@DNA cage core-shell structures. *ACS Nano* **2014**, *8*, 1130–1135.

[129] Li, Y. L.; Liu, Z. Y.; Yu, G. M.; Jiang, W.; Mao, C. D. Self-assembly of molecule-like nanoparticle clusters directed by DNA nanocages. *J. Am. Chem. Soc.* **2015**, *137*, 4320–4323.

[130] Zhou, C. Y.; Yang, Y. J.; Li, H. F.; Gao, F.; Song, C. Y.; Yang, D. L.; Xu, F.; Liu, N.; Ke, Y. G.; Su, S. et al. Programming surface-enhanced Raman scattering of DNA origami-templated metamolecules. *Nano Lett.* **2020**, *20*, 3155–3159.

[131] Martens, K.; Binkowski, F.; Nguyen, L.; Hu, L.; Govorov, A. O.; Burger, S.; Liedl, T. Long- and short-ranged chiral interactions in DNA-assembled plasmonic chains. *Nat. Commun.* **2021**, *12*, 2025.

[132] Zhang, Y. H.; Allen, A. C.; Petrek, Z. J.; Cao, H. H.; Kumar, D.; Goodlad, M. C.; Martinez, V. G.; Singh, J.; Zhang, J. Z.; Ye, T. Formation of linear plasmonic heterotrimers using nanoparticle docking to DNA origami cages. *J. Phys. Chem. C* **2024**, *128*, 11699–11708.

[133] Zhan, P. F.; Dutta, P. K.; Wang, P. F.; Song, G.; Dai, M. J.; Zhao, S. X.; Wang, Z. G.; Yin, P.; Zhang, W.; Ding, B. Q. et al. Reconfigurable three-dimensional gold nanorod plasmonic nanostructures organized on DNA origami tripod. *ACS Nano* **2017**, *11*, 1172–1179.

[134] Heck, C.; Kanehira, Y.; Kneipp, J.; Bald, I. Placement of single proteins within the SERS hot spots of self-assembled silver nanolenses. *Angew. Chem., Int. Ed.* **2018**, *57*, 7444–7447.

[135] Man, T. T.; Ji, W.; Liu, X. G.; Zhang, C.; Li, L.; Pei, H.; Fan, C. H. Chiral metamolecules with active plasmonic transition. *ACS Nano* **2019**, *13*, 4826–4833.

[136] Yeşilyurt, A. T. M.; Sanz-Paz, M.; Zhu, F. J.; Wu, X. F.; Sunil, K. S.; Acuna, G. P.; Huang, J. S. Unidirectional meta-emitters based on the kerker condition assembled by DNA origami. *ACS Nano* **2023**, *17*, 19189–19196.

[137] Liu, W. Y.; Li, L.; Yang, S.; Gao, J.; Wang, R. S. Self-assembly of heterogeneously shaped nanoparticles into plasmonic metamolecules on DNA origami. *Chemistry* **2017**, *23*, 14177–14181.

[138] Lee, J.; Huh, J. H.; Kim, K.; Lee, S. DNA origami-guided assembly of the roundest 60-100 nm gold nanospheres into plasmonic metamolecules. *Adv. Funct. Mater.* **2018**, *28*, 1707309.

[139] Sun, M. Y.; Xie, M.; Jiang, J. K.; Qi, Z. L.; Wang, L. H.; Chao, J. Customized self-assembled gold nanoparticle-DNA origami composite templates for shape-directed growth of plasmonic structures. *Nano Lett.* **2024**, *24*, 6480–6487.

[140] Vial, S.; Nykypanchuk, D.; Yager, K. G.; Tkachenko, A. V.; Gang, O. Linear mesostructures in DNA-nanorod self-assembly. *ACS Nano* **2013**, *7*, 5437–5445.

[141] Ma, W.; Kuang, H.; Xu, L. G.; Ding, L.; Xu, C. L.; Wang, L. B.; Kotov, N. A. Attomolar DNA detection with chiral nanorod assemblies. *Nat. Commun.* **2013**, *4*, 2689.

[142] Li, H. Y.; Park, S. H.; Reif, J. H.; LaBean, T. H.; Yan, H. DNA-templated self-assembly of protein and nanoparticle linear arrays. *J. Am. Chem. Soc.* **2004**, *126*, 418–419.

[143] Sharma, J.; Chhabra, R.; Cheng, A. C.; Brownell, J.; Liu, Y.; Yan, H. Control of self-assembly of DNA tubules through integration of gold nanoparticles. *Science* **2009**, *323*, 112–116.

[144] Ren, S. K.; Wang, J.; Song, C. Y.; Li, Q.; Yang, Y. J.; Teng, N.; Su, S.; Zhu, D.; Huang, W.; Chao, J. et al. Single-step organization of plasmonic gold metamaterials with self-assembled DNA nanostructures. *Research* **2019**, *2019*, 7403580.

[145] Lan, X.; Lu, X. X.; Shen, C. Q.; Ke, Y. G.; Ni, W. H.; Wang, Q. B. Au nanorod helical superstructures with designed chirality. *J. Am. Chem. Soc.* **2015**, *137*, 457–462.

[146] Tian, C.; Cordeiro, M. A. L.; Lhermitte, J.; Xin, H. L.; Shani, L.; Liu, M. Z.; Ma, C. L.; Yeshurun, Y.; DiMarzio, D.; Gang, O. Supra-nanoparticle functional assemblies through programmable stacking. *ACS Nano* **2017**, *11*, 7036–7048.

[147] Wang, P. F.; Huh, J. H.; Park, H.; Yang, D. L.; Zhang, Y. W.; Zhang, Y. L.; Lee, J.; Lee, S.; Ke, Y. G. DNA origami guided self-assembly of plasmonic polymers with robust long-range plasmonic resonance. *Nano Lett.* **2020**, *20*, 8926–8932.

[148] Lan, X.; Liu, T. J.; Wang, Z. M.; Govorov, A. O.; Yan, H.; Liu, Y. DNA-guided plasmonic helix with switchable chirality. *J. Am. Chem. Soc.* **2018**, *140*, 11763–11770.

[149] Xiao, S. J.; Liu, F. R.; Rosen, A. E.; Hainfeld, J. F.; Seeman, N. C.; Musier-Forsyth, K.; Kiehl, R. A. Selfassembly of metallic nanoparticle arrays by DNA scaffolding. *J. Nanopart. Res.* **2002**, *4*, 313–317.

[150] Le, J. D.; Pinto, Y.; Seeman, N. C.; Musier-Forsyth, K.; Taton, T. A.; Kiehl, R. A. DNA-templated self-assembly of metallic nanocomponent arrays on a surface. *Nano Lett.* **2004**, *4*, 2343–2347.
[151] Pinto, Y. Y.; Le, J. D.; Seeman, N. C.; Musier-Forsyth, K.; Taton, T. A.; Kiehl, R. A. Sequence-encoded self-assembly of multiple-nanocomponent arrays by 2D DNA scaffolding. *Nano Lett.* **2005**, *5*, 2399–2402.
[152] Zheng, J. W.; Constantinou, P. E.; Micheel, C.; Alivisatos, A. P.; Kiehl, R. A.; Seeman, N. C. Two-dimensional nanoparticle arrays show the organizational power of robust DNA motifs. *Nano Lett.* **2006**, *6*, 1502–1504.
[153] Zhang, J. P.; Liu, Y.; Ke, Y. G.; Yan, H. Periodic square-like gold nanoparticle arrays templated by self-assembled 2D DNA nanogrids on a surface. *Nano Lett.* **2006**, *6*, 248–251.
[154] Sharma, J.; Chhabra, R.; Liu, Y.; Ke, Y. G.; Yan, H. DNA-templated self-assembly of two-dimensional and periodical gold nanoparticle arrays. *Angew. Chem., Int. Ed.* **2006**, *45*, 730–735.
[155] Tang, J.; Ji, C.; Lu, X.; Cao, H. T.; Ling, Y. F.; Wu, Y. Q.; Qian, L. L.; He, Y.; Song, B.; Wang, H. Y. DNA origami plasmonic nanoantenna for programmable biosensing of multiple cytokines in cancer immunotherapy. *Anal. Chem.* **2024**, *96*, 9684–9692.
[156] Liu, W. Y.; Halverson, J.; Tian, Y.; Tkachenko, A. V.; Gang, O. Self-organized architectures from assorted DNA-framed nanoparticles. *Nat. Chem.* **2016**, *8*, 867–873.
[157] Wang, P. F.; Gaitanaros, S.; Lee, S.; Bathe, M.; Shih, W. M.; Ke, Y. G. Programming self-assembly of DNA origami honeycomb two-dimensional lattices and plasmonic metamaterials. *J. Am. Chem. Soc.* **2016**, *138*, 7733–7740.
[158] Wang, M. Y.; Dai, L. Z.; Duan, J. L.; Ding, Z. Y.; Wang, P.; Li, Z.; Xing, H.; Tian, Y. Programmable assembly of nano-architectures through designing anisotropic DNA origami patches. *Angew. Chem., Int. Ed.* **2020**, *59*, 6389–6396.
[159] Schreiber, R.; Santiago, I.; Ardavan, A.; Turberfield, A. J. Ordering gold nanoparticles with DNA origami nanoflowers. *ACS Nano* **2016**, *10*, 7303–7306.
[160] Yin, J.; Xie, M.; Wang, J. K.; Cui, M. R.; Zhu, D.; Su, S.; Fan, C. H.; Chao, J.; Li, Q.; Wang, L. H. Gold-nanoparticle-mediated assembly of high-order DNA nano-architectures. *Small* **2022**, *18*, 2200824.
[161] Nykypanchuk, D.; Maye, M. M.; van der Lelie, D.; Gang, O. DNA-guided crystallization of colloidal nanoparticles. *Nature* **2008**, *451*, 549–552.
[162] Park, S. Y.; Lytton-Jean, A. K. R.; Lee, B.; Weigand, S.; Schatz, G. C.; Mirkin, C. A. DNA-programmable nanoparticle crystallization. *Nature* **2008**, *451*, 553–556.
[163] Xiong, H. M.; Sfeir, M. Y.; Gang, O. Assembly, structure and optical response of three-dimensional dynamically tunable multicomponent superlattices. *Nano Lett.* **2010**, *10*, 4456–4462.
[164] Young, K. L.; Ross, M. B.; Blaber, M. G.; Rycenga, M.; Jones, M. R.; Zhang, C.; Senesi, A. J.; Lee, B.; Schatz, G. C.; Mirkin, C. A. Using DNA to design plasmonic metamaterials with tunable optical properties. *Adv. Mater.* **2014**, *26*, 653–659.
[165] Ross, M. B.; Ku, J. C.; Vaccarezza, V. M.; Schatz, G. C.; Mirkin, C. A. Nanoscale form dictates mesoscale function in plasmonic DNA-nanoparticle superlattices. *Nat. Nanotechnol.* **2015**, *10*, 453–458.
[166] Sun, L.; Lin, H. X.; Park, D. J.; Bourgeois, M. R.; Ross, M. B.; Ku, J. C.; Schatz, G. C.; Mirkin, C. A. Polarization-dependent optical response in anisotropic nanoparticle-DNA superlattices. *Nano Lett.* **2017**, *17*, 2313–2318.
[167] Tian, Y.; Lhermitte, J. R.; Bai, L.; Vo, T.; Xin, H. L.; Li, H. L.; Li, R. P.; Fukuto, M.; Yager, K. G.; Kahn, J. S. et al. Ordered three-dimensional nanomaterials using DNA-prescribed and valence-controlled material voxels. *Nat. Mater.* **2020**, *19*, 789–796.
[168] Tian, Y.; Zhang, Y. G.; Wang, T.; Xin, H. L.; Li, H. L.; Gang, O. Lattice engineering through nanoparticle-DNA frameworks. *Nat. Mater.* **2016**, *15*, 654–661.
[169] Shani, L.; Michelson, A. N.; Minevich, B.; Fleger, Y.; Stern, M.; Shaulov, A.; Yeshurun, Y.; Gang, O. DNA-assembled superconducting 3D nanoscale architectures. *Nat. Commun.* **2020**, *11*, 5697.
[170] Ji, M.; Zhou, Z. Y.; Cao, W. H.; Ma, N. N.; Xu, W. G.; Tian, Y. A universal way to enrich the nanoparticle lattices with polychrome DNA origami "homologs". *Sci. Adv.* **2022**, *8*, eadc9755.
[171] Zhang, T.; Hartl, C.; Frank, K.; Heuer-Jungemann, A.; Fischer, S.; Nickels, P. C.; Nickel, B.; Liedl, T. 3D DNA origami crystals. *Adv. Mater.* **2018**, *30*, 1800273.
[172] Xu, Y. N.; Zhang, Q.; Chen, R. Z.; Cao, H. T.; Tang, J.; Wu, Y. Q.; Lu, X.; Chu, B. B.; Song, B.; Wang, H. Y. et al. NIR-II photoacoustic-active DNA origami nanoantenna for early diagnosis and smart therapy of acute kidney injury. *J. Am. Chem. Soc.* **2022**, *144*, 23522–23533.
[173] Khan, I.; Saeed, K.; Khan, I. Nanoparticles: Properties, applications and toxicities. *Arab. J. Chem.* **2019**, *12*, 908–931.
[174] Zhu, J. J.; Wu, F.; Han, Z. H.; Shang, Y. X.; Liu, F. S.; Yu, H. Y.; Yu, L.; Li, N.; Ding, B. Q. Strong light-matter interactions in chiral plasmonic-excitonic systems assembled on DNA origami. *Nano Lett.* **2021**, *21*, 3573–3580.